A LOW REYNOLDS NUMBER FLOW PROBLEM WITH APPLICATION TO SPERMATOZOAN TRANSPORT IN CERVICAL MUCUS

by

RONALD E. SMELSER

B.S.M.E., University of Cincinnati

(1971)

SUBMITTED IN PARTIAL FULFILLMENT

OF THE REQUIREMENTS FOR THE

DEGREE OF MASTER OF SCIENCE

at the

MASSACHUSETTS INSTITUTE OF TECHNOLOGY

September 1972

Signature redacted

Signature of Author.....
Department of Mechanical Engineering, August 14, 1972

Signature redacted

Certified by.....
Thesis Supervisors

Signature redacted

Accepted by.....
Chairman, Departmental Committee on Graduate Students

A LOW REYNOLDS NUMBER FLOW PROBLEM

WITH APPLICATION TO SPERMATOZOAN TRANSPORT

IN CERVICAL MUCUS

by

Ronald E. Smelser

Submitted to the Department of Mechanical Engineering on August 14, 1972 in partial fulfillment of the requirements forthe degree of Master of Science in Mechanical Engineering.

ABSTRACT

Sperm transport in the human cervix is a vital step in the process of fertilization and the roles of the cervix and the cervical mucus have been extensively discussed and investigated. A mechanism to explain sperm transport through the cervical mucus has been suggested by E. Odeblad. The cervical mucus was found to consist of large macromolecules suspended in a water-like fluid. At mid-cycle, the time of maximum fertility, these molecules align themselves and according to Odeblad oscillate because of thermal agitation. According to Odeblad this alignment of the macromolecules furnishes channels of low viscosity fluid through which the sperm may pass with relative ease aided by the oscillations of the macromolecules.

A mathematical model of Odeblad's proposed mechanism of sperm transport in the cervix is presented which idealizes the geometry as a self-propelling infinite sheet in a two-dimensional channel. The sheet propels itself by propagating waves of lateral displacement. The channel walls are allowed to vibrate as proposed by Odeblad as right traveling waves, left traveling waves or standing waves. The propulsive velocity and energy expended by the sheet and flow rates in the channel are computed. These results are presented and conclusions are given concerning the effect of wall oscillations on self propelling sheets. The conclusions of Odeblad's theory are contrasted with the results of the model.

Thesis supervisors: Thomas J. Lardner, William J. Shack

Titles: Associate Professor of Mechanical Engineering
Assistant Professor of Mechanical Engineering

Acknowledgments

I would like to thank Professor Shack for his endless patience and guidance throughout this investigation. I am also grateful for the probing questions of Professor Lardner which brought about the completion of this work. To both, thank you for the insights which were given and for the encouragement and the friendship which made this year an enjoyable experience.

Special thanks go to my parents and my fiancé, Barbara, who have made this endeavor worthwhile.

I would also like to thank M.I.T., The Ford Foundation and The National Science Foundation for their financial support through this year.

Table of Contents

Introduction

The passage of spermatozoa through the human cervix is a vital step in the process of fertilization. Sperm deposited in the vagina must pass through the mucus filling the cervix. The mechanism of transport in the cervix and the function of the cervix in fertility has been the subject of much recent research (Davajan, et.al., 1970; Moghissi and Blandau, 1972).

A survey of current literature examining the structure and function of the cervix and its secretions is presented. *In vitro* and *in vivo* experimental studies of sperm transport to explain at times conflicting observed phenomena are also discussed.

One mechanism, proposed by Odeblad (1962), has attempted to explain the rate of passage of sperm through the cervical mucus. The mucus has been shown to be anisotropic. This anisotropy is caused by long chain molecules. These macromolecules align themselves at midcycle and, according to Odeblad, vibrate. Odeblad (1962) suggests that the vibration aids the passage of sperm through the cervical mucus plug.

A mathematical model is formulated to investigate the hydrodynamics of this theory. An idealized geometry of an infinite sheet in a two-dimensional channel is used. The channel is assumed to be symmetric with waves on the walls. The sheet, representing the sperm, is propelled by passing waves down itself. This propulsion was first shown to be possible in low Reynolds number flow by G. I. Taylor (1951).

Using this model, results are obtained for the propulsive velocity of the sheet, the energy dissipated by the sheet, and the flow rate in the channel. For the case of zero amplitude wall motion, the solution reduces

to results presented by Reynolds (1965) for an oscillating sheet between flat rigid walls. Also, the present solution has overcome the questions of uniqueness which Reynolds did not resolve.

Finally, a discussion of the analysis is given in view of Odeblad's (1962) theory, and alternative mechanisms are considered for sperm transport through the cervix.

Section I: Structure and Function of Cervical Mucus

The role of the cervix and of the cervical mucus in sperm transport has been the object of much investigation and controversy. In this section, a review of some important aspects of cervical structure and the properties of the cervical mucus is presented. A discussion of *in vitro* measurements of sperm penetration in cervical mucus and evidence for the active and the passive role of the cervix in transport is also given. The section concludes with a discussion of an interesting theory due to Odeblad, who assigns an active role to the components of cervical mucus in sperm transport. This theory provides the motivation for the hydrodynamic study which follows in Section II. Additional reviews of the role of the cervix in sperm transport are presented by Davajan, et. al. (1970), Moghissi (1969, 1971), and Sobrero (1963). (A bibliography has been prepared by Reproduction Research Information, Ltd., 1970).

The uterine cervix is a complex anatomical structure. The epithelium is composed of secretory and ciliated cells (Hafez and Kanagawa, 1972). The secretory cells are grouped in crypts or clefts resembling gland-like structures (see Fig. I-1). These secretory sites are not glands but rather an extension of the endocervical mucosa (Moghissi, 1972). It has been reported that there are approximately 100 of these crypts lining the cervix (Odeblad, 1966). These clefts may run longitudinally, transversely or obliquely, but they will never cross each other (Moghissi, 1972).

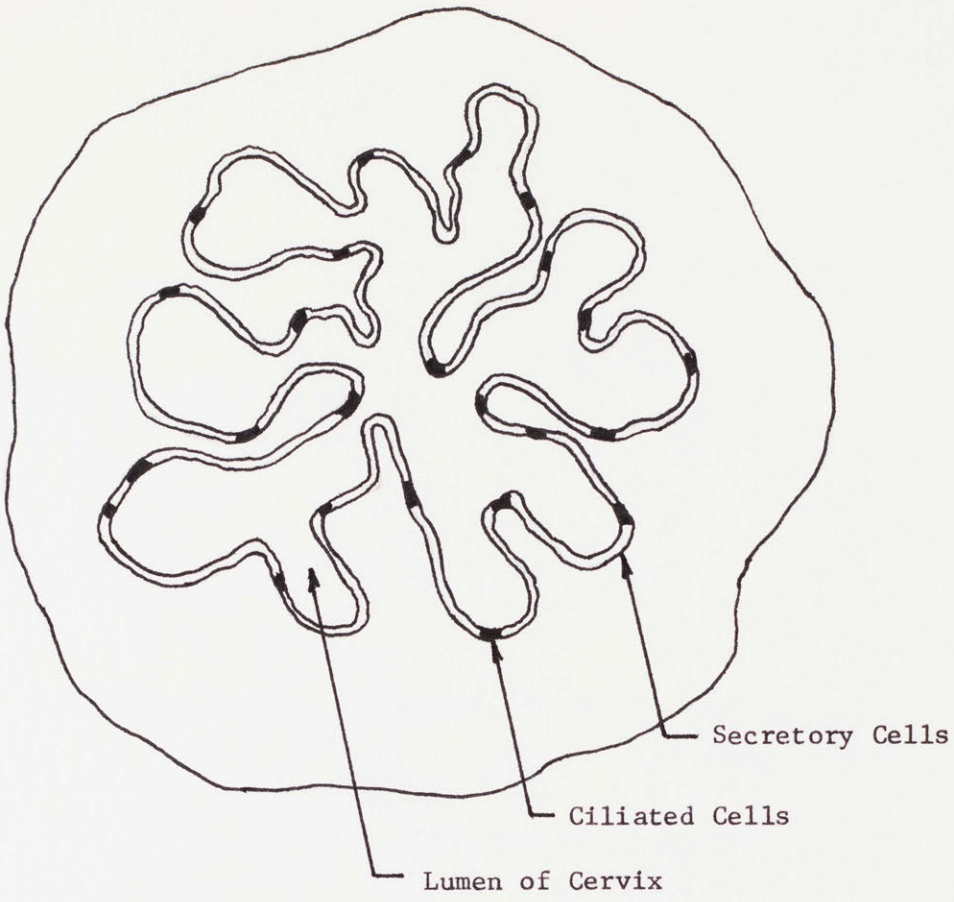

Fig. I-1

Also, these structures are responsible for the creation of the mucus filling the cervical lumen (Sobrero, 1969).

According to a recent study by Hafez and Kanagawa (1972), the ciliated cells are arranged singly or in groups. These cells contain well-developed kinocilia and comprise about 5% - 9% of the cervical epithelia. When observed in tissue culture, the cilia are seen to beat with an effective stroke which is toward the vagina (Fig. I-2). The principal function of the ciliated cells seems to be the transport of the secreted mucus into the cervical lumen (Hafez and Kanagawa, 1972).

The structure and secretory activity of the cervix undergo cyclic changes in response to hormonal stimulation of the ovaries (Fig. I- 3).

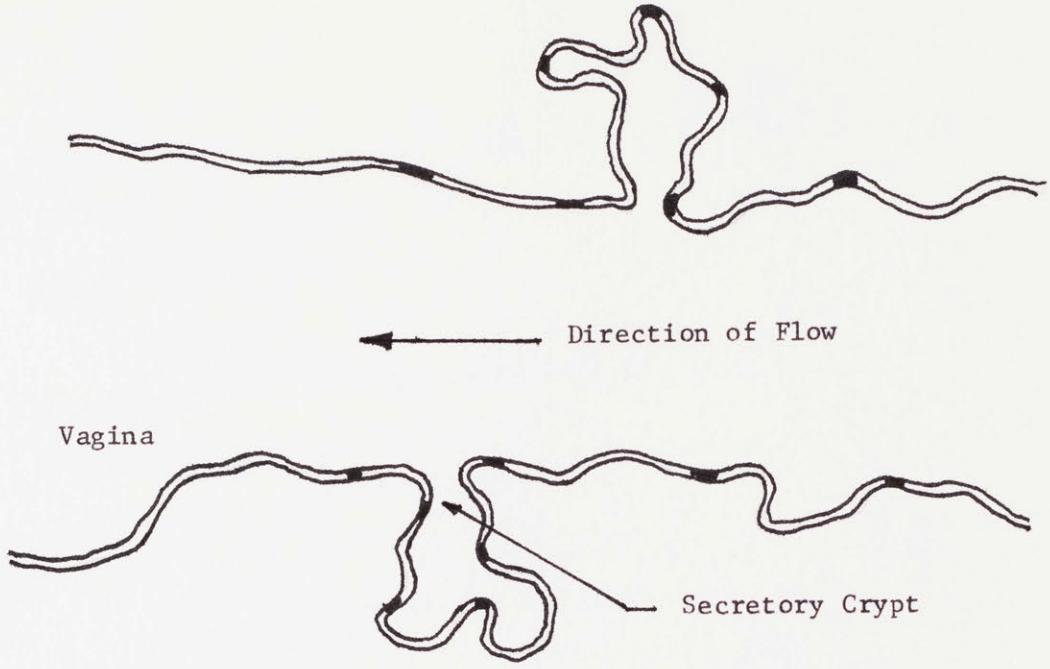

Fig. I-2

During the preovulatory phase of the cycle, estrogen production increases. The external os of the cervix is seen to dilate under this influence (Bergman, 1953; Marcus and Marcus, 1968; Odeblad, 1966; Sobrero, 1969). The cervical mucus also undergoes changes in chemical composition and in physical properties such as spinnbarkeit and viscosity. (Spinnbarkeit is the ability of the mucus to be drawn into threads). During the normal menstrual cycle, the thread length can range from 1 cm. preovulation to 15 cm. near ovulation (Moghissi, 1966). Karni, et.al. (1971) measured the Newtonian viscosity through the cycle and found a sizeable decrease to occur near ovulation. These findings are in agreement with Odeblad's (1966)

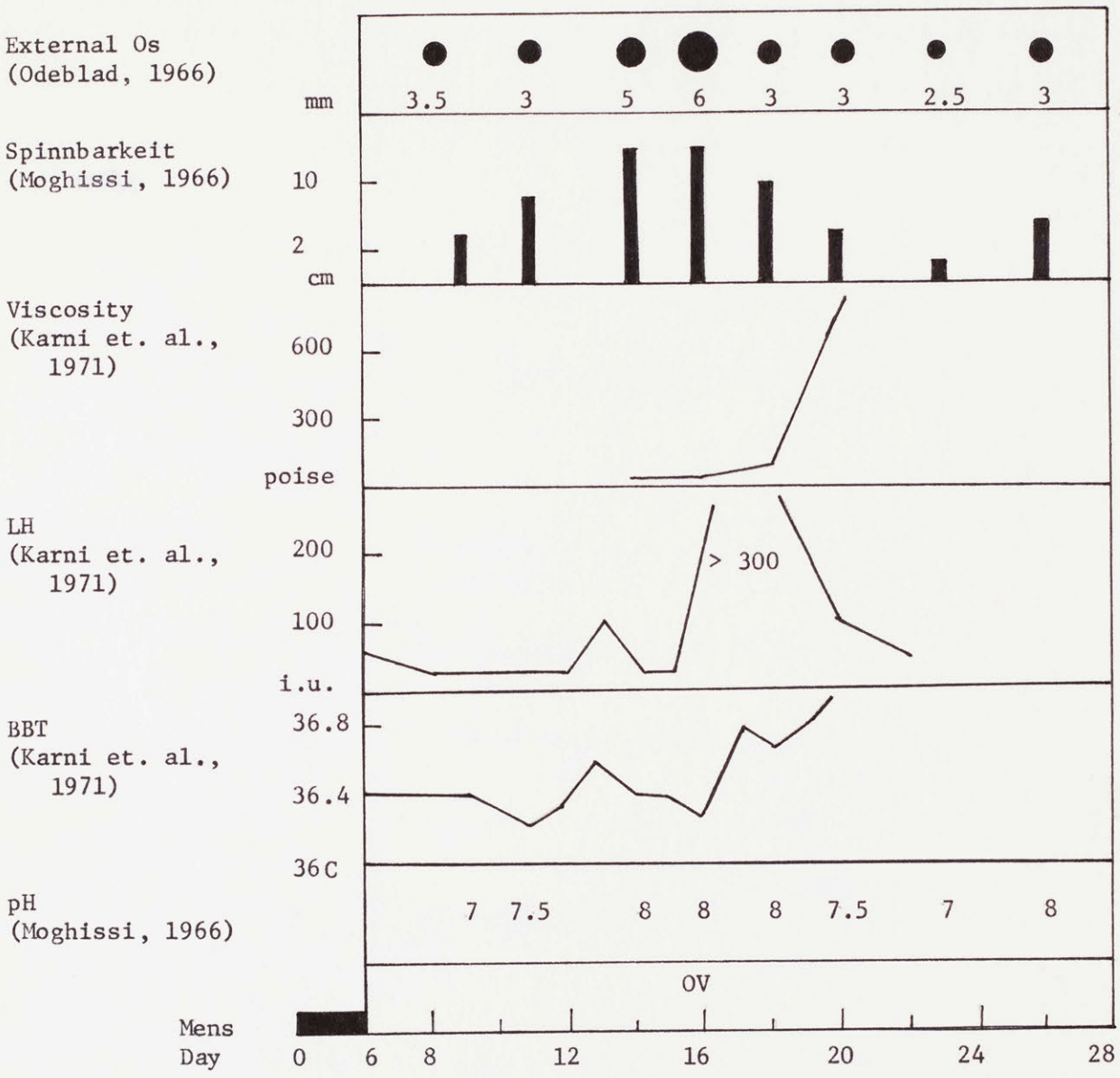

Fig. I-3

data and the qualitative observations of Moghissi (1966) and others. Karni, et. al. (1971) also found that the decrease in viscosity of the mucus correlated with the basal body temperature rise (BBT) and the luteinizing hormone (LH) surge, thus acting as an indicator of ovulation.

Corresponding to the observed physical properties of mucus, Odeblad (1969) has identified five types of cervical secretion. These are summarized in Table I-1. Since sperm penetration is of greatest importance at

E	Estrogenic Preovulatory Mucus
G	Gestrogenic, Postovulatory Mucus
H	
H_1	Virginal Mucorrhea (more free-flowing than Type E)
H_2	Prolonged Estrogenic Treatment
H_3	Intense Estrogenic Treatment
Q	Chronic Inflammatory Conditions
V	Accute Inflammatory Conditions

Table I-1

or near ovulation, attention will be centered on Type E and G mucus. In the preovulatory phase, the mucus secretion becomes clear, watery, and translucent (Bergman, 1953; Gibbons and Mattner, 1966; Moghissi, 1972; Sobrero, 1967). The volume of mucus produced rises from the 20-60 mg/day postovulatory to a possible maximum of 700 mg/day (Moghissi, 1972). Accompanying the rise in mucus production, Schumacher (1970) has observed changes in the biochemistry of cervical mucus.

The study of the biochemistry of cervical mucus has led to the identification of two components. These have been designated the low viscosity and high viscosity portions. Studies of the low viscosity component have shown it to consist of soluble inorganic salts, low molecular weight sugars, and serum proteins dissolved in water (Davajan, et. al., 1970; Elstein and MacDonald, 1970; Moghissi and Syner, 1970; Schumacher, 1970; Odeblad and Rosenberg, 1968). The high viscosity component of cervical mucus is a gel-like substance consisting of two glycoproteins as well as albumin (Moghissi and Syner, 1970).

An understanding of sperm penetration through the cervical mucus is of prime importance in the study of fertility. Two in vitro tests are now in use to evaluate sperm penetrability in samples of cervical mucus. These are the Kremer Test and the Miller-Kurzrok Test (Davajan, et. al, 1970). The Kremer Test consists of drawing mucus into a capillary tube and placing the tube vertically in a reservoir of semen (Davajan, et. al., 1970) (Fig. I-4). The movement of the sperm into the capillary tube is then observed.

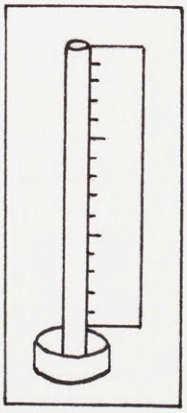

Kremer Test

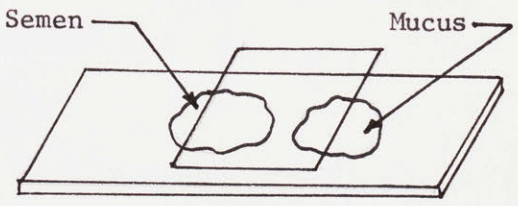

Miller-Kurzrok Test

Fig. I-4

The Miller-Kurzrok Test is a slide technique. In this test mucus is placed in a drop on the slide. Semen is deposited adjacent to it and a cover slip is carefully placed on top so as not to mix the specimens (Davajan, et. al., 1970) (Fig. I-4).

The swimming rate of sperm in cervical mucus has been determined using the above penetration tests. The results of these tests are summarized in Table I-2. Carlborg's (1969) results, using a Kremer technique, are reported for two cases. The first is for data obtained from randomly

Investigator	Speed (μ/sec)
Belenoshkin (1960)	33
Carlborg (1969)	17 - 35 45
Elstein and MacDonald (1970)	30
Harvey (1960)	32 and 59
Most Reported Average (Davajan, et.al., 1970)	33 - 55

Table I-2

collected samples of cervical mucus. The second result is from earlier tests performed on ovulatory mucus. The results of Harvey (1960) and Elstein and MacDonald (1970) were obtained using a slide test with mid-cycle mucus. All results fell near the most reported averages of Davajan, et. al., (1970). For the reported speeds in Table I-2, sperm could move through the cervix, 25 mm in length (Carlborg, 1969), on their own motility in approximately 15 minutes.

It is generally accepted (see, e.g., Davajan, et.al., 1970) that sperm transport through the upper portion of the uterus and Fallopian tubes is too rapid to be accounted for solely by the motility of the sperm. If only transport through the cervix is considered, the question is more controversial. Several observers have reported accelerated transport through the cervix and have proposed mechanisms by which this can be achieved.

Sobrero and McCleod (1962) noted that sperm were present in the cervical mucus of patients within 90 to 180 seconds after ejaculation. These observations indicate almost immediate penetration of sperm into cervical mucus. The first few drops of ejaculated semen are known to contain the highest concentrations of sperm (Blandau, 1969; Sobrero and McCleod, 1962). In attempting to explain the rapid passage of sperm into the mucus, Sobrero and McCleod (1962) postulate the following explanation

> Sexual intercourse...results in a back-and-forth movement of mucus from cervix to vagina, where the mucus comes into intimate contact with the semen even though they do not appear to mix. These movements of the cervical mucus may well account for the early appearance of spermatozoa in the mucus of the cervical canal.

Inward and outward movement of the mucus plug has also been reported by Belonoshkin (1960), who attributed it not to the action of the penis but to female orgasm. (Sobrero (1967) could not confirm this finding.) This movement of mucus has been designated as "insuck". Belonoshkin (1960) noted that in patients who had not achieved orgasm sperm were not present in the mucus column. However, in those who had, sperm were found at a depth of 1 to 1.5 centimeters in the cervical mucus, within 1 to 3 minutes. On the basis of the average rate of penetration, 1 cm. in 5 minutes, Belonoshkin (1960) concludes that sperm would not be able to reach that depth on their own motility in such a short time. He also notes that orgasm is not necessary for penetration to occur.

Fox and Fox (1969) have indicated that during coitus contractions of the uterus and vagina are observed. In a subsequent investigation, Fox, et.al. (1970) introduced a rapid telemetric pressure transducer into the uterus. Pressure recordings were made of the uterine contractions during female orgasm. Their work showed a pressure drop of 26 cm. of H_2O occurred in the uterus. This drop in pressure was sustained for approximately 2 minutes and flow of mucus into the cervix should be possible. Enhorning, et.al. (1963) recorded such retrograde flow in women of normal reproductive age. This they concluded could account for the transport of sperm once they had penetrated the mucus. Trapal (Davajan, et.al, 1970) was able to recover caramine particles in the endometrial cavity after they had been placed in the vagina prior to coitus without a cervical cap. This also suggests a retrograde flow in the cervix.

In an effort to determine if the cervix plays an active role in sperm transport, various experiments have been conducted using inert particles (Blandau, 1969; Davajan, et.al., 1970; de Boer, 1972; Egli and Newton, 1961; Sobrero, 1963,1967). These results are summarized in Table I-3.

Egli and Newton (1961) placed a suspension of carbon particles approximately the size of spermatozoa in the posterior fornix of three patients. Each patient was near ovulation and was injected with oxytocin, a hormone known to cause uterine contractions. Two of the three cases revealed carbon particles had been transported to the tubes within one half hour after deposition. Their results were not conclusive since the anesthetic may have dilated the external os.

de Boer (1971) attempted to confirm the findings of Egli and Newton (1961). The results were negative in all but one case. (In this case the patient had a lacerated cervix.) He then suggested that a lowering of

Investigator	Number of Subjects	Transport	No Transport
de Boer			
Vagina	18	1	17
Injection into Cervix (all phases of cycle)	56	17	39
Egli and Newton	3	2	1
Sobrero			
Radiopaque material (1963,1967)	11	--	3 (M,O)
		Sperm	Material
Radiopaque materal and sperm	9	3(M,O)	3(M,O)
		6(C)	6(C)

M = Masturbation
C = Coitus
O = Orgasm

Table I-3

abdominal pressure may have been responsible for the findings of Egli and Newton (1961).

In another set of experiments, de Boer (1971) attempted to find out if particles could be transported once in the cervix. He injected a suspension of carbon particles into the cervix and found after hysterectomy, that particles were present in the uterus. These findings were not conclusive, however, since force was required to inject the suspension into the cervix and may have caused the particles to move into the uterus. Based on his findings, de Boer (1971) concluded that sperm motility was essential to

pass through the cervix; however, once in the upper genital tract, sperm could be transported by the activity of the tract.

Sobrero (1963, 1967) conducted experiments using radiopaque materials and a mixture of radiopaque material and sperm in a cervical cap. In all cases, no sign of the inert material was detected above the vagina with or without orgasm.

Fox and Fox (1967) have raised objections to findings based on the use of cervical caps and inert materials. They feel that the method and material used are not natural and should not be expected to simulate intercourse. They suggest a cup placed over the cervix may cause the os to become smaller and thus prevent normal passage into the cervix.

Although the bulk of the evidence suggests that inert particles are not transported by the cervix, it is possible that the cervix and its secretions may play an "active" role in augmenting sperm transport. Moghissi (1968) has shown that the presence of cervical mucus is necessary if sperm are to pass from the vagina into the uterus. Using excised uteri, he placed the external os of the cervix in semen. In six cases sperm were found in cervices containing mucus. For two cases in which the mucus was absent, no sperm were found.

Other mechanisms of accelerated transport through the cervix which have been presented may be due to pH variations or the formation of phalanges. As shown in Fig. I-3, the pH of cervical mucus undergoes cyclic changes. These variations have been measured by MacDonald and Lumley (1970) and Moghissi (1966). These findings are important because sperm are rendered inactive in an acid environment, (pH 6.5, Moghissi, et.al.,1964 ; Harvey, 1960). Moghissi (1971) indicates that the maximal speed of sperm can be expected at a pH of 8.25. This corresponds to the pH value at midcycle.

Moghissi, et.al.(1964) noted in slide penetration tests that cervical mucus, when placed in contact with semen, forms fingerlike projections which they have denoted as phalanges. These projections form what appear to be entrance points for the sperm to cross the interface between semen and cervical mucus. The phalanges increase the area of contact and trap pockets of semen in the mucus. They feel that the phenomenon may account for the observation of Egli and Newton (1961). This seems unlikely, however, since the phalanges are microscopic and will not extend large distances into the mucus.

Gibbons and Mattner (1966, 1971) have suggested that the cervix aids in sperm transport by functioning as a reservoir for sperm. Based on observations of bovine mucus, they suggest that the cervix is a receptacle for the slow release of sperm into the uterus (Gibbons and Mattner, 1966). The sperm move along the lines of strain of the mucus and into the cervical crypts (Gibbons and Mattner, 1971). Preliminary work of Hafez and Kanagawa (1971) is in agreement with the hypothesis. From the cervical crypts, sperm slowly break through the glycoprotein and move into the uterus (Gibbons and Mattner, 1971).

The storage also functions as a method of selecting sperm. The motile sperm are the only ones which are able to move into the crypts (Gibbons and Mattner, 1971). The non-motile sperm are eliminated.

Odeblad (1959, 1968) has made a detailed study of the physical structure of cervical mucus. Using nuclear magnetic resonance (NMR) he found cervical mucus to be anisotropic with something resembling free water between the macromolecules (Odeblad, 1959). The viscosity of this substance is about 0.03 poise. (Odeblad, 1962).

The cervical crypts secrete the long molecules which group together and form micelles. This gives rise to "... two physiologically relevant directions within the mucus plug, namely upward and downward."(Odeblad, 1962). The distance at midcycle between the micelles is 1 - 10μ while the diameter is 0.5μ (Odeblad, 1968). In the luteal phase, the mucus is a close mesh with a spacing of about 0.3μ (Fig. I-5).

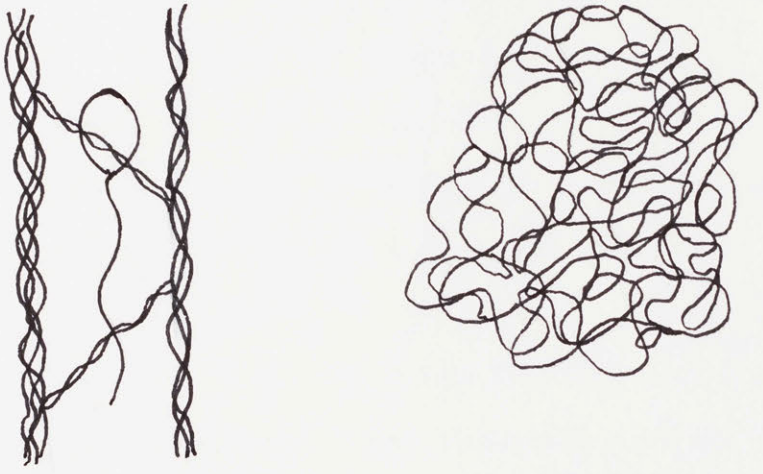

Midcycle Luteal

Fig. I-5

Tampion and Gibbons (1962) provided additional evidence for this structure with their observations that bull sperm would swim in oriented patterns. They took oestrus bovine mucus and stretched it onto a slide. Bull sperm were pipetted on to one end of the mucus strand and the slide was incubated. After incubation the sperm were examined and found to be moving in the direction of elongation of the mucus. They reasoned that since the mucus was anisotropic the stretching caused the molecules to align directionally. To check the results sperm were placed in saline and

also into glycoprotein suspended in saline. In both cases the sperm swam in random fashion (Tampion and Gibbons, 1962). Carlborg (1969) also observed that in capillary tests for penetration, sperm always tended to migrate along the axis of the capillary tube. He also noticed that if the mucus were pushed back and forth in the tube, orderly penetration was disrupted. This led him to the conclusion that aspiration of the mucus into the tube caused the alignment of macromolecules.

Additional direct evidence for this structure was furnished by Elstein, Mitchell, and Syrett (1971) using electron microscopy, and by Davajan, et.al. (1971) who observed aligned fern-like patterns when midcycle mucus was stretched on slides and allowed to dry. Both teams of investigators observed luteal phase mucus to be tightly meshed, thus visually confirming Odeblad's structure.

Odeblad (1962) has presented an interesting theory of the "active" function of the cervix based on these observations of the structure of the mucus. To account for the bulk deformability of the mucus, the macromolecules must be flexible. "As a consequence of this flexibility, the macromolecular system must necessarily execute molecular movements of some kind, owing to the thermal agitation which is present everywhere." (Odeblad, 1962.)

He suggests that the vibration of midcycle micelle segments can be analyzed as a harmonic oscillator with fixed ends. He concludes that this corresponds to a standing wave on the micelle. Since the segment is assumed to be in thermal equilibrium with the surrounding fluid, the oscillations must have a frequency spectrum similar to that of water. The motion is then thought to be composed of two waves, one traveling up the micelle,

the other down. He then postulates a type of "resonance" interaction,

> ... There is also a frequency band fitting the sperm tail undulation frequency, thus allowing the micelle to act as a kind of ladder for the tail when it exerts its propelling action. The micelle vibrations also give rise to propagating distentions of the intramicellar spaces conveying the spermatozoa through the cervical mucus with a minimum of hydrodynamic resistance. (Odeblad, 1971).

"This can be explained as a type of mechanical resonance between tail frequency and thermal oscillation frequency of the molecular lattice"(Odeblad, 1968). Odeblad concludes that such a model " ... makes it feasible that the migration of a spermatozoon occurs without exhaustion ... " (Odeblad, 1962). It will also "... bring about a separation of morphologically or functionally normal from defective spermatozoa ... " (Odeblad, 1962), and "... may facilitate exchange of oxygen, carbon dioxide, glucose, and other diffusible metabolites ..." (Odeblad, 1962).

Davajan, et. al. (1970), in presenting Odeblad's theory, state, "In vivo, the role of the cilia lining the entire endocervical canal has been totally ignored. It is well known that the cilia in a specific organ beat in a propagating manner. This oscillation (beat) created by wave propagation may be more than sufficient to account for the energy required to maintain oscillations in the cervical mucus." In view of the findings of Hafez and Kanagawa (1972), the low number of ciliated cells in the cervical epithelia makes it unlikely that a wave could effectively propagate down the cervical canal furnishing energy to the oscillations, and thus the oscillations, if they exist, must be of thermal origin as Odeblad has suggested.

A mathematical model, which may give some insight into the interaction between a sperm and the vibrating micelles which Odeblad (1962) has postulated, is presented in the next section. This model is used to investigate the possibility that sperm transport is enhanced by the transfer of energy from the oscillating micelle to the sperm.

Section II: Hydrodynamic Analysis

The first analysis of swimming microorganisms was carried out by G. I. Taylor (1951). In this work, he estimated the Reynolds number for a spermatozoon to be (Taylor, 1951),

$$Re = \frac{\text{Inertial Stress}}{\text{Viscous Stress}} \approx 10^{-6}$$

This indicates that the viscous stresses are much greater than the inertia stresses, and so the inertia stresses can be neglected. The spermatozoon was modeled as a two-dimensional doubly infinite sheet down which waves propagated. The oscillation was considered to have the form (Fig. II-1),

$$y = b \sin k(x - ct)$$

where

y = vertical coordinate

x = horizontal coordinate

b = amplitude of the sheet

k = wave number

c = phase velocity

t = time

relative to an observer fixed to the moving sheet. (Taylor, 1951).

Fig. II-1

Taylor (1951) assumed the sheet was inextensible (see Appendix I) and found the propulsive velocity to fourth order to be

$$\frac{V_p}{c} = \frac{1}{2} b^2k^2(1 - \frac{19}{16} b^2k^2).$$

Drummond (1966) also considered small amplitude periodic waves of arbitrary shape and extended Taylor's result to eighth order.

In an attempt to consider more realistic geometries, Taylor (1952) in a later paper assumed the shape of the body to be that of a cylindrical filament. Waves of displacement were assumed to pass down the filament and a propulsive velocity was determined. Hancock (1953) removed Taylor's (1952) restriction that the disturbance be of small amplitude. Furthermore, Hancock modeled the sperm as a slender filament of non-zero thickness. By placing a distribution of Stokeslets and doublets along the centerline

of the filament, Hancock was able to satisfy the boundary conditions of the problem and determine the velocity of propulsion. In the limiting case as the amplitude became small relative to the wave length, the result was found to agree with Taylor (1951, 1952) to order b^2k^2 for both zero thickness and non-zero thickness filaments.

The analysis of Hancock (1953) was followed by the work of Gray and Hancock (1955). Their method for determining the propulsive velocity used constant drag coefficients suggested by the results of Hancock. The unknown propulsive velocity of the filament was determined by requiring the force on the filament to be zero.

To investigate the propulsion of sperm in a bounded fluid, Reynolds (1965) proposed a two-dimensional model. The model consisted of a doubly infinite sheet swimming between rigid walls equidistant from the mean plane of the sheet (Fig. II-2).

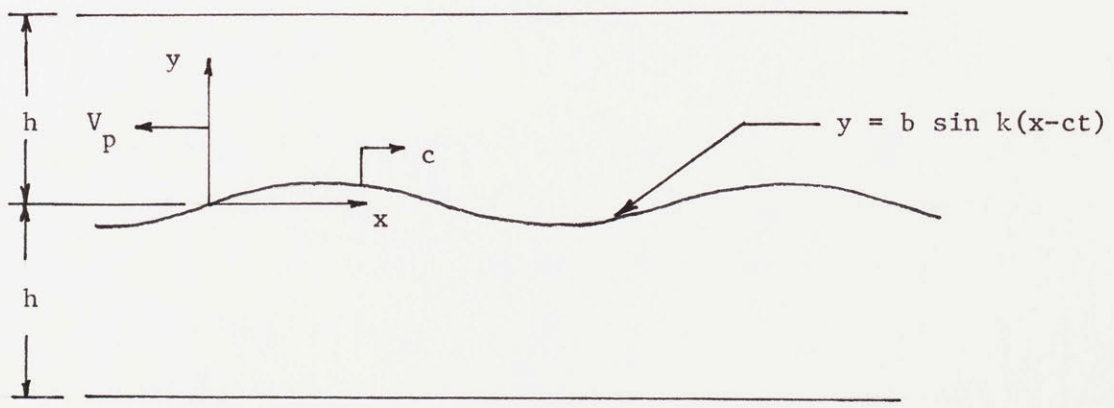

Fig. II-2

The sheet was assumed to pass waves of lateral displacement down itself. The form of the waves in a frame moving with the sheet was assumed to be

$$y = b \sin k(x - ct) .$$

The boundary conditions on the sheet were determined as given in Appendix I.

For this geometry, Reynolds (1965) found the propulsive velocity to depend on both the parameters bk and kh. To second order in bk, propulsive velocity is given by

$$\frac{V_p}{c \frac{b^2k^2}{2}} = \frac{V_p}{V_\infty} = \frac{\sinh^2(kh) + k^2h^2}{\sinh^2(kh) - k^2h^2}$$

where

V_∞ = Propulsive velocity in an infinite medium for a sheet motion of the same amplitude

The rate of energy dissipation per wavelength by the sheet is

$$\frac{W}{2b^2k^3c^2\mu} = \frac{W}{W_\infty} = \frac{\cosh(kh)\sinh(kh) + kh}{\sinh^2(kh) - k^2h^2} + O(\alpha^3)$$

where

W_∞ = Rate of energy dissipated in an infinite medium

Fig. II-3 gives a sketch of $\frac{V_p}{V_\infty}$ and $\frac{W}{W_\infty}$ as a function of kh. As kh becomes small, the velocity increases without bound. However, the energy output per wavelength also becomes infinite. A more realistic estimate of the wall effect would be to ask how the velocity varies with kh for a fixed energy output of the sheet. To maintain a constant dissipation rate as kh becomes small, the amplitude of the sheet must decrease while k, μ, and c are held constant. For a fixed energy output W, the ratio

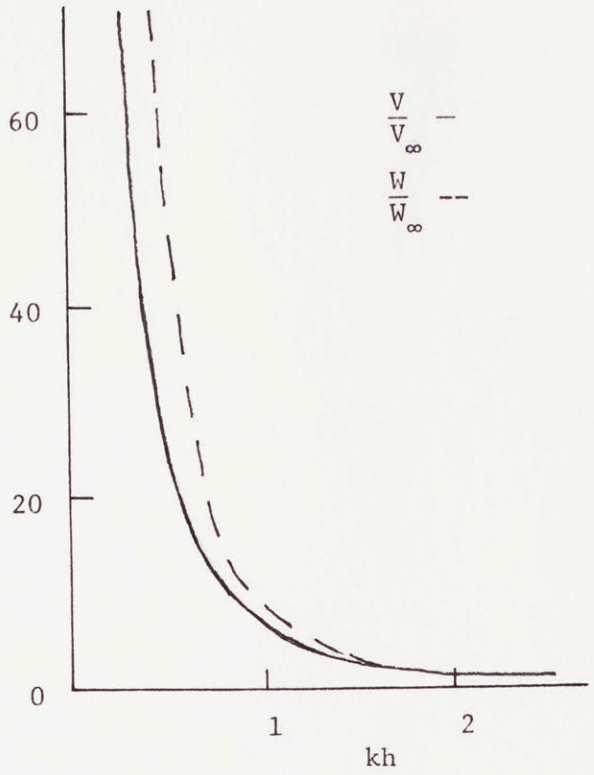

Fig. II-3

of the velocity of a sheet in a channel to that of a sheet in an infinite media is given by

$$\left.\frac{V_p}{V_\infty}\right|_{\text{fixed } W} = \frac{\sinh^2(kh) + k^2h^2}{\cosh(kh)\sinh(kh) + kh} .$$

The ratio of $\frac{V_p}{V_\infty}$ is shown in Fig. II-4. It is seen that for equal energy dissipation rates in bounded and unbounded fluids, the propulsive velocity in a channel can be increased above the velocity in an infinite fluid. An optimum channel spacing does exist for a fixed energy expenditure and produces a 10% increase in velocity.

In view of Reynolds' (1965) results, the question was posed: Can an oscillating wall give an increase in velocity greater than that predicted by the analysis of Reynolds (1965)? An analysis of this question should furnish insight into the hypothesis Odeblad has proposed for sperm

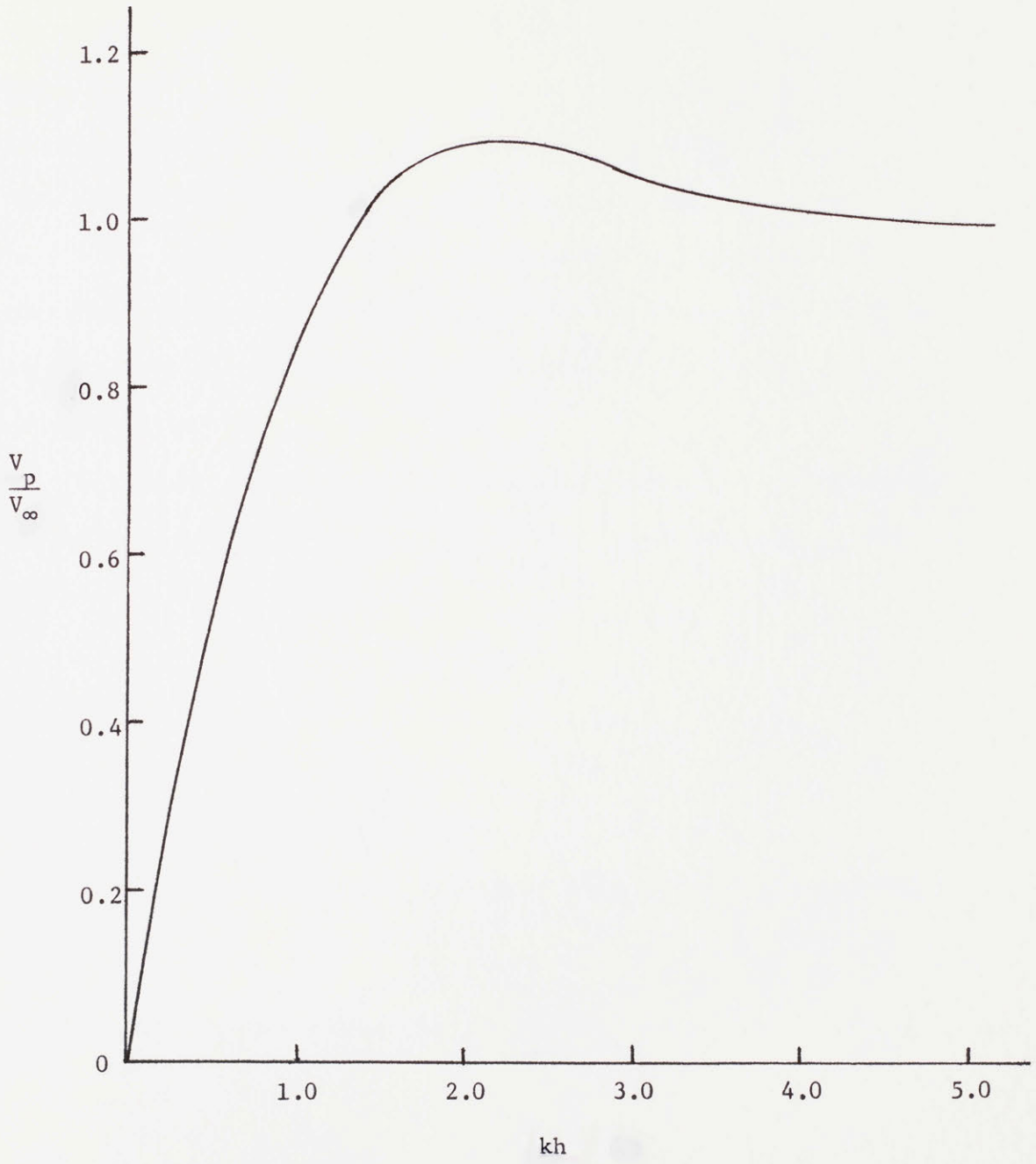

Fig. II-4

transport through the cervix as discussed in Section I. A two-dimensional model similar to that of Reynolds (1965) (Fig. II-2) was chosen for the analysis. The walls of the channel were allowed to oscillate and the sheet was assumed to move by passing sinusoidal waves down itself. Based on the observation of Tuck (1968), (for further discussion of this boundary condition, see Appendix I), the waves on sheet are assumed to be "peristaltic" in nature and the computation is carried to second order in $\alpha = bk$. The proposed model is postulated to investigate whether the phenomena proposed by Odeblad may exist. The model is not intended to furnish quantitative results on the actual speed of propulsion of sperm through the cervix.

In pseudo steady flows with vanishingly small Reynolds numbers, the equations of motion, the Navier-Stokes equations, reduce to (Illingsworth, 1963)

$$\mu \nabla^2 \underset{\sim}{u} = \nabla p \qquad (1)$$

where

$\underset{\sim}{u}$ = velocity vector

p = pressure

when conservation of mass for an incompressible fluid is satisfied

$$\nabla \cdot \underset{\sim}{u} = 0 . \qquad (2)$$

For two-dimensional problems, we can define a stream function ψ such that

$$u = -\frac{\partial \psi}{\partial y} \quad , \quad v = \frac{\partial \psi}{\partial x} \qquad (3)$$

where

u = x - Direction velocity

v = y - Direction velocity

ψ = Stream function

and continuity is satisfied identically. Taking the curl of (1) and substituting (3) for u and v, we obtain

$$\mu \nabla \times \nabla^2 \underset{\sim}{u} = \nabla \times \nabla p = 0 \qquad (4)$$

or

$$\nabla^4 \psi = 0 \qquad (5)$$

where in rectangular coordinates

$$\nabla^4 = \frac{\partial^4}{\partial x^4} + 2 \frac{\partial^4}{\partial x^2 \partial y^2} + \frac{\partial^4}{\partial y^4} \cdot$$

Equation (5) is the governing equation in terms of the stream function for low Reynolds number flow.

The boundaries of the flow field are similar to that of Reynolds (1965). The sheet is assumed to oscillate about y = 0 while the mean plane of oscillation of the walls is at y = $\pm$ h (Fig. II-5).

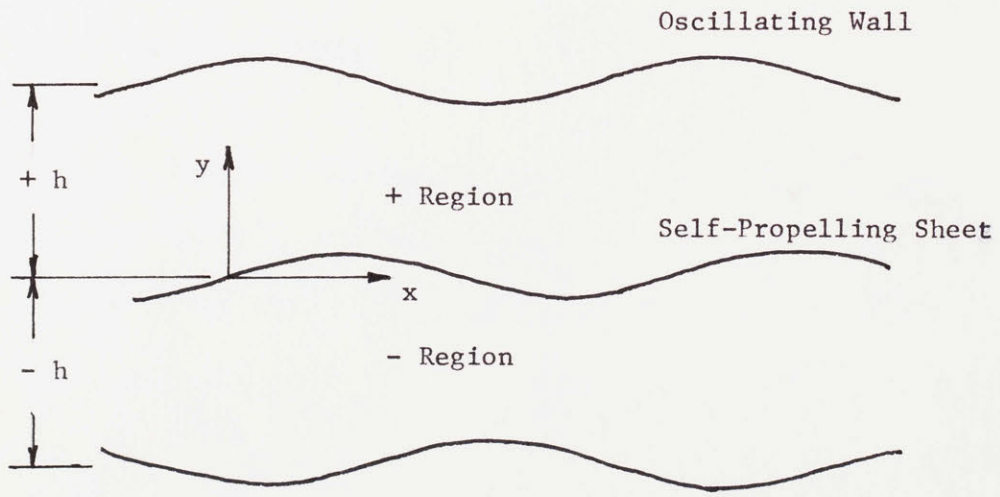

Fig. II-5

In a fixed frame, the wall undergoes a peristaltic wave motion. The sheet is assumed to be a peristaltic wave relative to an observer fixed on the moving sheet. At the walls and the sheet, the fluid is required to satisfy the no-slip condition. For propulsion with negligible inertia effect, the total force on the sheet must vanish. This condition was not used by Reynolds (1965), and led to difficulties concerning the uniqueness of his solution. To determine the total force, it is necessary to know the stream function in regions above and below the sheet.

A solution to the governing equation (5) was sought subject to the no-slip conditions and the zero force condition on the sheet. The solution was carried out in the form of an asymptotic series. An expression for the propulsive velocity in terms of the wall parameters, sheet parameters, and spacing was found. In the present analysis three cases for the wall motion were considered. They were:

1) Waves traveling in the direction of motion of the waves of the sheet.
2) Waves traveling in a direction opposite to the direction of motion of the waves of the sheet.
3) Standing waves.

The analysis will be carried out for case 1, while case 2 and case 3 will be analyzed in Appendices A-VIII and A-IX.

The forms of the wall and the sheet in the fixed frame, Frame 1, are

$$y_{w1}^{*\pm} = \pm h^{*} \pm b_w \sin k_w(x_1^{*} - c_w t^{*})$$

$$y_{s1}^{*} = b_s \sin k_s [x_1^{*} - (c_s - V_p^{*})t^{*}] \qquad (6)$$

Introducing the following dimensionless variables,

$$
\begin{aligned}
y &= k_s y^* & h &= k_s h^* & v &= \frac{v^*}{c_s} \\
x &= k_s x^* & V_p &= \frac{V_p^*}{c_s} & m &= \frac{k_w}{k_s} \\
t &= k_s c_s t^* & u &= \frac{u^*}{c_s} & \beta &= \frac{b_w}{b_s} \\
p &= \frac{1}{\mu c k} p^* & \psi &= \frac{k}{c} \psi^* & \alpha &= b_s k_s \\
 & & & & \gamma &= \frac{c_w}{c_s}
\end{aligned}
\qquad (7)
$$

The Navier-Stokes equations have the dimensionless form using (7) and (1)

$$\nabla^2 \underset{\sim}{u} = \nabla p \qquad (8)$$

And in terms of the dimensionless stream function equation (5) becomes

$$\nabla^4 \psi = 0 \qquad (9)$$

The non-dimensional form of the wall and sheet are (Fig. II-6)

$$
\begin{aligned}
y_{w_1}^{\pm} &= \pm h \pm \alpha\beta \sin m(x_1 - \gamma t) \\
y_{s_1} &= \alpha \sin [x - (1 - V_p)t].
\end{aligned}
\qquad (10)
$$

The solution will be sought in two regions, an upper (+) region and a lower (-) region. Since the particles on the wall undergo a periodic motion, the velocity of particles on the wall, as in the case of peristaltic pumping, is given by

$$u_{w_1}^{\pm} = 0, \quad v_{w_1}^{\pm} = \frac{\partial y_{w_1}^{\pm}}{\partial t} = \mp \alpha\beta \, m \, \gamma \cos m(x_1 - \gamma t) \qquad (11)$$

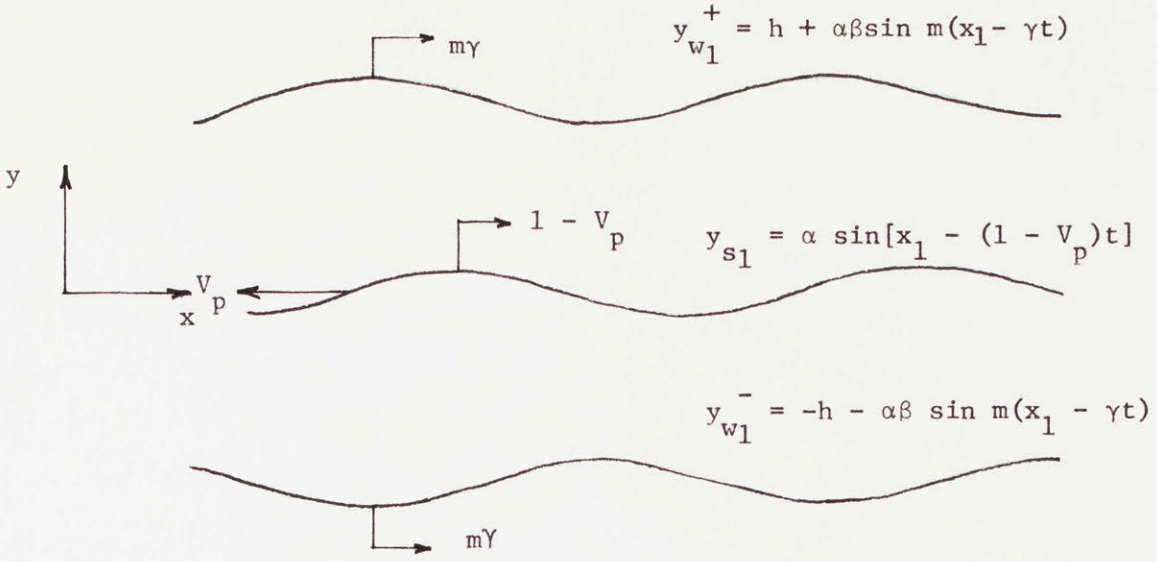

Fig. II-6

In a frame, 2, moving with the sheet at velocity $-V_p$, the sheet is seen to undergo simple sinusoidal motion. Velocity and coordinate transformations give,

$$\begin{aligned} u_1 &= u_2 - V_p \quad , \quad x_1 = x_2 - V_p t \\ v_1 &= v_2 \quad , \quad y_1 = y_2 \end{aligned} \tag{12}$$

The velocity V_p has been assumed constant. This assumption will be verified when V_p is determined. Applying equations (12) to (10) and (11) we obtain (Fig. II-7)

$$u_{w_2}^{\pm} = V_p \ , \ v_{w_2}^{\pm} = \mp \alpha\beta \ m \ \gamma \cos m[x_2 - (\gamma + V_p)t]$$

$$y_{w_2}^{\pm} = \pm h \pm \alpha\beta \sin m[x_2 - (\gamma + V_p)t] \tag{13}$$

$$y_s = \alpha \sin (x_2 - t)$$

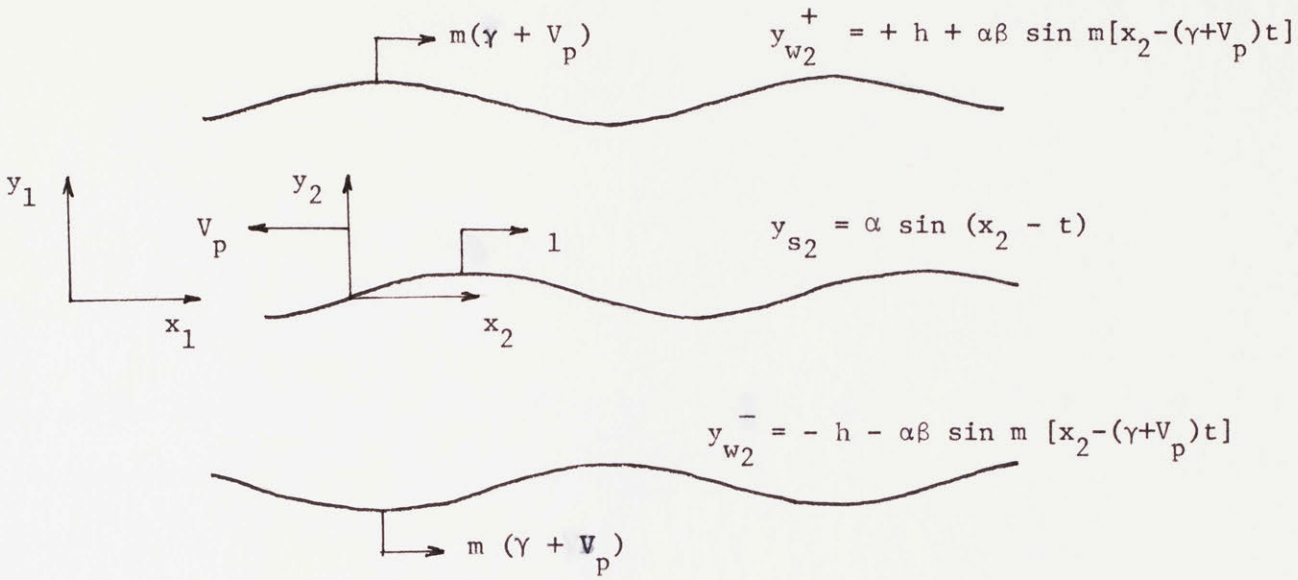

Fig. II-7

The velocity of particles on the sheet is now found to be (see Appendix I)

$$u_{s_2} = 0, \quad v_{s_2} = \frac{\partial y_{s2}}{\partial t} = -\alpha \cos(x_2 - t) \qquad (14)$$

Finally, for an observer moving relative to Frame 2 with a speed 1 (the non-dimensional phase velocity of the wave), the sheet is brought to rest. The transformation equations for this frame, 3, are

$$\begin{aligned} u_2 &= u_3 + 1 \quad , \quad x_2 = x_3 + t \\ v_2 &= v_3 \quad , \quad y_2 = y_3 \end{aligned} \qquad (15)$$

Using equations (15) with (13) and (14) the velocities of particles on the sheet and wall in Frame 3 are

$$u_{w_3}^{\pm} = V_p - 1 \ , \ v_{w_3}^{\pm} = \mp \alpha\beta \ m \ \gamma \cos m[x_3 - (\gamma + V_p - 1)t]$$

$$u_{s_3}^{\pm} = -1 \qquad , \ v_{s_3}^{\pm} = -\alpha \cos x_3. \tag{16}$$

The boundary shapes are given by (Fig. II-8).

$$y_{w_2}^{\pm} = \pm h \pm \alpha\beta \sin m[x_3 - (\gamma + V_p - 1)t]$$

$$y_{s_3} = \alpha \sin x_3 \tag{17}$$

Since the inertia terms in the Navier-Stokes Equations have been neglected, the governing equation (5) for ψ is invariant under these coordinate transformations.

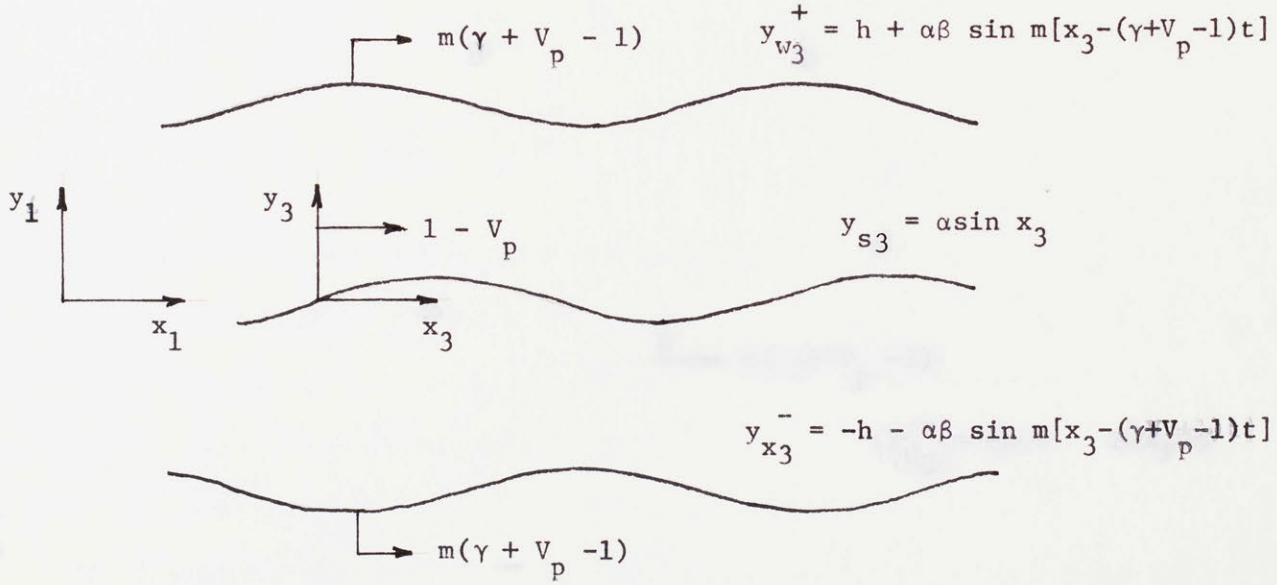

Fig. II-8

The kinematic boundary conditions for ψ are given by the no-slip velocity condition on the sheet and wall. Dropping the subscript denoting the frame, these are from (16)

$$
\begin{aligned}
u_{w}^{\pm} &= -\left.\frac{\partial \psi^{\pm}}{\partial y}\right|_{y_{w}^{\pm}} = V_{p} - 1 \\
v_{w}^{\pm} &= \left.\frac{\partial \psi^{\pm}}{\partial x}\right|_{y_{w}^{\pm}} = \mp \alpha\beta\, m\, \gamma \cos m\,[x - (\gamma + V_{p} - 1)t] \\
u_{s} &= -\left.\frac{\partial \psi^{\pm}}{\partial y}\right|_{y_{s}} = -1 \\
v_{s} &= \left.\frac{\partial \psi^{\pm}}{\partial x}\right|_{y_{s}} = -\alpha \cos x
\end{aligned}
\tag{18}
$$

where V_{p} is yet to be determined.

Since we are neglecting the inertial terms, the viscous force on the top and bottom of the sheet must equal zero,

$$
\int_{y_{s}} (\underset{\sim}{T}^{+} + \underset{\sim}{T}^{-})\, ds = 0 \tag{19}
$$

For this reason it is necessary as noted previously to determine the solution in the two regions above and below the sheet.

To obtain a unique solution for the flow field, it is necessary to specify the external pressure difference applied to ends of the channel. In this analysis, we assume that there is no imposed pressure gradient.

The boundary conditions are to be evaluated on the sinusoidal boundary shapes of the sheet and the walls. Equations (18) can be expanded in Taylor series about their respective mean planes of oscillation:

$$\frac{\partial \psi}{\partial y}^{\pm}\Big|_{y_w^{\pm}} = \frac{\partial \psi}{\partial y}^{\pm}\Big|_{\pm h} + \frac{\partial^2 \psi}{\partial y^2}^{\pm}\Big|_{\pm h}(y_w^{\pm} \mp h) + \frac{1}{2}\frac{\partial^3 \psi}{\partial y^3}^{\pm}\Big|_{\pm h}(y_w^{\pm} \mp h)^2 + \cdots$$

$$\frac{\partial \psi}{\partial x}^{\pm}\Big|_{y_w^{\pm}} = \frac{\partial \psi}{\partial x}^{\pm}\Big|_{\pm h} + \frac{\partial^2 \psi}{\partial x \partial y}^{\pm}\Big|_{\pm h}(y_x^{\pm} \mp h) + \frac{1}{2}\frac{\partial^3 \psi}{\partial x \partial y^2}^{\pm}\Big|_{\pm h}(y_w^{\pm} \mp h)^2 + \cdots$$

$$\frac{\partial \psi}{\partial y}\Big|_{y_s} = \frac{\partial \psi}{\partial y}^{\pm}\Big|_{0} + \frac{\partial^2 \psi}{\partial y^2}^{\pm}\Big|_{0}(y_s) + \frac{1}{2}\frac{\partial^3 \psi}{\partial y^3}^{\pm}\Big|_{0}(y_s)^2 + \cdots \tag{20}$$

$$\frac{\partial \psi}{\partial x}^{\pm}\Big|_{y_s} = \frac{\partial \psi}{\partial x}^{\pm}\Big|_{0} + \frac{\partial^2 \psi}{\partial x \partial y}^{\pm}\Big|_{0}(y_s) + \frac{1}{2}\frac{\partial^3 \psi}{\partial x \partial y^2}^{\pm}\Big|_{0}(y_s)^2 + \cdots$$

where y_s and $y_w^{\pm}$ are given by (17). Expanding $y_w^{\pm}$ by a trigonometric addition formula, we obtain

$$\begin{aligned} y_w^{\pm} &= \pm h \pm \alpha\beta \sin m[x - (\gamma + V_p - 1)t] \\ y_w^{\pm} &= \pm h \pm \alpha\beta\,(\tilde{F} \sin mx + \tilde{G} \cos mx) \end{aligned} \tag{21}$$

with

$$\tilde{F} = \cos m(1 - \gamma - V_p)t$$

$$\tilde{G} = \sin m(1 - \gamma - V_p)t$$

Similarly, the velocity at the wall can be expanded

$$\begin{aligned} v_w^{\pm} &= \mp \alpha\beta\, m\, \gamma \cos m[x - (\gamma + V_p - 1)t] \\ &= \mp \alpha\beta\, m\, \gamma(\tilde{F} \cos mx - \tilde{G} \sin mx) \end{aligned} \tag{22}$$

Substituting y_s, (17), and $y_w^{\pm}$, (21), into (20), and equating (20) to the velocities on the boundary, (18) and (22), yields

$$\frac{\partial\psi}{\partial y}^{\pm}\Big|_0 + \frac{\partial^2\psi}{\partial y^2}^{\pm}\Big|_0 (\alpha \sin x) + \frac{1}{2}\frac{\partial^3\psi}{\partial y^3}^{\pm}\Big|_0 (\alpha \sin x)^2 + \cdots = 1$$

$$\frac{\partial\psi}{\partial x}^{\pm}\Big|_0 + \frac{\partial^2\psi}{\partial x\partial y}^{\pm}\Big|_0 (\alpha \sin x) + \frac{1}{2}\frac{\partial^3\psi}{\partial x\partial y^2}^{\pm}\Big|_0 (\alpha \sin x)^2 + \cdots$$

$$= -\alpha \cos x$$

$$\frac{\partial\psi}{\partial y}^{\pm}\Big|_{\pm h} + \frac{\partial^2\psi}{\partial y^2}^{\pm}\Big|_{\pm h} [\pm \alpha\beta (\tilde{F} \sin mx + \tilde{G} \cos mx)] \tag{23}$$

$$+ \frac{1}{2}\frac{\partial^3\psi}{\partial y^3}\Big|_{\pm h} [\pm \alpha\beta (\tilde{F} \sin mx + \tilde{G} \cos mx)]^2 + \cdots = 1-V_p$$

$$\frac{\partial\psi}{\partial x}^{\pm}\Big|_{\pm h} + \frac{\partial^2\psi}{\partial x\partial y}^{\pm}\Big|_{\pm h} [\pm \alpha\beta (\tilde{F} \sin mx + \tilde{G} \cos mx)] +$$

$$+ \frac{1}{2}\frac{\partial^3\psi}{\partial x\partial y^2}^{\pm}\Big|_{\pm h} [\pm \alpha\beta (\tilde{F} \sin mx + \tilde{G} \cos mx)]^2 + \cdots$$

$$= \mp \alpha\beta m \gamma (\tilde{F} \cos mx - \tilde{G} \sin mx).$$

A solution to

$$\nabla^4\psi = 0 \tag{9}$$

and the above boundary conditions will be found in the form of an asymptotic series. A convenient non-dimensional parameter, $\alpha = b_s k_s$, the product of the amplitude and the wave number of the sheet, is suggested by the boundary conditions. Since V_p is also unknown, it, too, must be expanded in a series in α. The series approximations are

$$\psi^{\pm} = \psi_0^{\pm} + \alpha\psi_1^{\pm} + \alpha^2\psi_2^{\pm} + O(\alpha^3) \tag{24}$$

and

$$V_p = V_{p0} + \alpha V_{p1} + \alpha^2 V_{p2} + O(\alpha^3). \tag{25}$$

Upon substitution of (24) into (9), we find

$$\nabla^4\psi_0^{\pm} + \alpha\nabla^4\psi_1^{\pm} + \alpha^2\nabla^4\psi_2^{\pm} + 0(\alpha^3) = 0 \tag{26}$$

For (26) to be satisfied for all α, each term multiplying α must vanish identically. This leads to the following sequence of equations for the ψ's to order α^2.

$$\nabla^4\psi_0 = \nabla^4\psi_1 = \nabla^4\psi_2 = 0 \tag{27}$$

Similarly, the substitution of (24) and (25) into the kinematic boundary conditions (23) yield,

$$\frac{\partial}{\partial y}\left[\psi_0^{\pm} + \alpha\psi_1^{\pm} + \alpha^2\psi_2^{\pm} + 0(\alpha^3)\right]\Big|_0 + \frac{\partial^2}{\partial y^2}\left[\psi_0^{\pm} + \alpha\psi_1^{\pm} + \alpha^2\psi_2^{\pm} + 0(\alpha^3)\right]\Big|_0 (\alpha\sin x)$$

$$+ \frac{1}{2}\frac{\partial^3}{\partial y^2}\left[\psi_0^{\pm} + \alpha\psi_1^{\pm} + \alpha^2\psi_2^{\pm} + 0(\alpha^3)\right]\Big|_0 (\alpha \sin x)^2 + \cdots = 1$$

$$\frac{\partial}{\partial x}\left[\psi_0^{\pm} + \alpha\psi_1^{\pm} + \alpha^2\psi_2^{\pm} + 0(\alpha^3)\right]\Big|_0 + \frac{\partial^2}{\partial x\partial y}\left[\psi_0^{\pm} + \alpha\psi_1^{\pm} + \alpha^2\psi_2^{\pm} + 0(\alpha^3)\right]\Big|_0 (\alpha\sin x)$$

$$+ \frac{1}{2}\frac{\partial^3}{\partial x\partial y^2}\left[\psi_0^{\pm} + \alpha\psi_1^{\pm} + \alpha^2\psi_2^{\pm} + 0(\alpha^3)\right]\Big|_0 (\alpha \sin x)^2 + \cdots = -\alpha\cos x$$

$$\frac{\partial}{\partial y}\left[\psi_0^{\pm} + \alpha\psi_1^{\pm} + \alpha^2\psi_2^{\pm} + 0(\alpha^3)\right]\Big|_{\pm h} + \frac{\partial^2}{\partial y^2}\left[\psi_0^{\pm} + \alpha\psi_1^{\pm} + \alpha^2\psi_2^{\pm} + 0(\alpha^3)\right]\Big|_{\pm h}$$

$$\times\left[\pm\alpha\beta\,(\widetilde{F}\sin mx + \widetilde{G}\cos mx)\right] + \frac{1}{2}\frac{\partial^3}{\partial y^2}\left[\psi_0^{\pm} + \alpha\psi_1^{\pm} + \alpha^2\psi_2^{\pm} + 0(\alpha^3)\right]\Big|_{\pm h}$$

$$\times\left[\pm\alpha\beta\,(\widetilde{F}\sin mx + \widetilde{G}\cos mx)\right]^2 + \cdots = 1 - \left[V_{p0} + \alpha V_{p1} + \alpha^2 V_{p2} + 0(\alpha^3)\right] \tag{28}$$

$$\frac{\partial}{\partial x}\left[\psi_0^{\pm} + \alpha\psi_1^{\pm} + \alpha^2\psi_2^{\pm} + 0(\alpha^3)\right]\Big|_{\pm h} + \frac{\partial^2}{\partial x\partial y}\left[\psi_0^{\pm} + \alpha\psi_1^{\pm} + \alpha^2\psi_2^{\pm} + 0(\alpha^3)\right]\Big|_{\pm h}$$

$$\times\left[\pm\alpha\beta\,(\widetilde{F}\sin mx + \widetilde{G}\cos mx)\right] + \frac{1}{2}\frac{\partial^3}{\partial x\partial y^2}\left[\psi_0^{\pm} + \alpha\psi_1^{\pm} + \alpha^2\psi_2^{\pm} + 0(\alpha^3)\right]\Big|_{\pm h}$$

$$\times\left[\pm\alpha\beta\,(\widetilde{F}\sin mx + \widetilde{G}\cos mx)\right]^2 = \mp\alpha\beta\, m\,\gamma\,(\widetilde{F}\cos mx - \widetilde{G}\sin mx)$$

Equating like powers of α, we obtain the kinematic boundary conditions for ψ_0, ψ_1, ψ_2:

$$\left.\frac{\partial \psi_0}{\partial y}\right|_0 = 1$$

$$\left.\frac{\partial \psi_0}{\partial x}\right|_0 = 0$$

$$\left.\frac{\partial \psi_0}{\partial y}\right|_{\pm h} = 1 - V_{p0} \tag{29}$$

$$\left.\frac{\partial \psi_0}{\partial x}\right|_{\pm h} = 0$$

$$\left.\frac{\partial \psi_1}{\partial y}\right|_0 = -\left.\frac{\partial^2 \psi_0}{\partial y^2}\right|_0 \sin x$$

$$\left.\frac{\partial \psi_1}{\partial x}\right|_0 = -\cos x - \left.\frac{\partial^2 \psi_0}{\partial x \partial y}\right|_0 \sin x$$

$$\left.\frac{\partial \psi_1}{\partial y}\right|_{\pm h} = -V_{p1} \mp \beta \left.\frac{\partial^2 \psi_0}{\partial y^2}\right|_{\pm h} (\tilde{F} \sin x + \tilde{G} \cos x) \tag{30}$$

$$\left.\frac{\partial \psi_1}{\partial x}\right|_{\pm h} = \mp \beta m \gamma (\tilde{F} \cos mx - \tilde{G} \sin mx)$$

$$\mp \beta \left.\frac{\partial^2 \psi_0}{\partial x \partial y}\right|_{\pm h} (\tilde{F} \sin mx + \tilde{G} \cos mx)$$

$$\left.\frac{\partial \psi_2}{\partial y}^{\pm}\right|_0 = -\left.\frac{\partial^2 \psi_1}{\partial y^2}^{\pm}\right|_0 \sin x - \frac{1}{2}\left.\frac{\partial^3 \psi_0}{\partial y^3}^{\pm}\right|_0 \sin^2 x$$

$$\left.\frac{\partial \psi_2}{\partial x}^{\pm}\right|_0 = -\left.\frac{\partial^2 \psi_1}{\partial x \partial y}^{\pm}\right|_0 \sin x - \frac{1}{2}\left.\frac{\partial^3 \psi_0}{\partial x \partial y^2}^{\pm}\right|_0 \sin^2 x$$

$$\left.\frac{\partial \psi_2}{\partial y}^{\pm}\right|_{\pm h} = -V_{p2} \mp \beta \left.\frac{\partial \psi^2_1}{\partial y^2}^{\pm}\right|_{\pm h} (\tilde{F} \sin mx + \tilde{G} \cos mx)$$

$$-\beta^2 \frac{1}{2}\left.\frac{\partial^3 \psi_0}{\partial y^3}^{\pm}\right|_{\pm h} (\tilde{F} \sin mx + \tilde{G} \cos mx)^2 \qquad (31)$$

$$\left.\frac{\partial \psi_2}{\partial x}^{\pm}\right|_{\pm h} = \mp \beta \left.\frac{\partial^2 \psi_1}{\partial x \partial y}^{\pm}\right|_{\pm h} (\tilde{F} \sin mx + \tilde{G} \cos mx)$$

$$-\beta^2 \frac{1}{2}\left.\frac{\partial^3 \psi_0}{\partial x \partial y^2}^{\pm}\right|_{\pm h} (\tilde{F} \sin mx + \tilde{G} \cos mx)^2$$

The equilibrium condition must also be expanded in a manner similar to the kinematic boundary conditions (see Appendix A-II). These conditions are given by

$$\int_{-\infty}^{\infty} (\tau_{xy}^{(0)+} - \tau_{xy}^{(0)-})\Big|_0 dx = 0$$

$$\int_{-\infty}^{\infty} (\tau_{yy}^{(0)+} - \tau_{yy}^{(0)-})\Big|_0 dx = 0 \qquad (32)$$

$$\int_{-\infty}^{\infty} [(\tau_{yx}^{(1)+} - \tau_{yx}^{(1)-}) - \cos x\,(\tau_{xx}^{(0)+} - \tau_{xx}^{(0)-}) + \sin x \frac{\partial}{\partial y}(\tau_{yx}^{(0)+} - \tau_{yx}^{(0)-})]\Big|_0 dx = 0 \tag{33}$$

$$\int_{-\infty}^{\infty} [(\tau_{yy}^{(1)+} - \tau_{yy}^{(1)-}) - \cos x\,(\tau_{xy}^{(0)+} - \tau_{xy}^{(0)-}) + \sin x \frac{\partial}{\partial y}(\tau_{yy}^{(0)+} - \tau_{yy}^{(0)-})]\Big|_0 dx = 0$$

$$\int_{-\infty}^{\infty} [(\tau_{yx}^{(2)+} - \tau_{yx}^{(2)-}) - \cos x(\tau_{xx}^{(1)+} - \tau_{xx}^{(1)-}) + \tfrac{1}{2}\sin^2 x \frac{\partial^2}{\partial y^2}(\tau_{yx}^{(0)+} - \tau_{yx}^{(0)-}) + \sin x \frac{\partial}{\partial y}(\tau_{yx}^{(1)+} - \tau_{yx}^{(1)-}) - \sin x \cos x\,(\tau_{xx}^{(0)+} - \tau_{xx}^{(0)-})]\Big|_0 dx=0 \tag{34}$$

$$\int_{-\infty}^{\infty} [(\tau_{yy}^{(2)+} - \tau_{yy}^{(2)-}) - \cos x\,(\tau_{xy}^{(1)+} - \tau_{xy}^{(1)-}) + \tfrac{1}{2}\sin^2 x \frac{\partial^2}{\partial y^2}(\tau_{yy}^{(0)+} - \tau_{yy}^{(0)-}) + \sin x \frac{\partial}{\partial y}(\tau_{yy}^{(1)+} - \tau_{yy}^{(1)-}) - \sin x \cos x\,(\tau_{xy}^{(0)+} - \tau_{xy}^{(0)-})]\Big|_0 dx = 0$$

where the stresses are given by

$$\begin{aligned}
\tau_{xx}^{(n)\pm} &= -p_n^{\pm} - 2\frac{\partial^2 \psi_n^{\pm}}{\partial x \partial y} \\
\tau_{yy}^{(n)\pm} &= -p_n^{\pm} + 2\frac{\partial^2 \psi_n^{\pm}}{\partial y \partial x} \\
\tau_{xy}^{(n)\pm} = \tau_{yx}^{(n)\pm} &= -\frac{\partial^2 \psi_n^{\pm}}{\partial y^2} + \frac{\partial^2 \psi_n^{\pm}}{\partial x^2} \\
\frac{\partial p_n^{\pm}}{\partial x} &= -\frac{\partial^3 \psi_n^{\pm}}{\partial x^2 \partial y} - \frac{\partial^3 \psi_n^{\pm}}{\partial y^3} \\
\frac{\partial p_n^{\pm}}{\partial y} &= \frac{\partial^3 \psi_n^{\pm}}{\partial x^3} + \frac{\partial^3 \psi_n^{\pm}}{\partial y^2 \partial x}
\end{aligned} \tag{35}$$

For the zeroth order solution, the governing equation (27) and the boundary conditions (29) and (32) are

$$\nabla^4 \psi_0^{\pm} = 0 \tag{27}$$

$$\begin{aligned}
&\left.\frac{\partial \psi_0^{\pm}}{\partial y}\right|_0 = 1 \\
&\left.\frac{\partial \psi_0^{\pm}}{\partial x}\right|_0 = 0 \\
&\left.\frac{\partial \psi_0^{\pm}}{\partial y}\right|_{\pm h} = 1 - V_p \\
&\left.\frac{\partial \psi_0^{\pm}}{\partial x}\right|_{\pm h} = 0
\end{aligned} \tag{29}$$

$$\begin{aligned}
&\int_{-\infty}^{\infty} \left.(\tau_{yx}^{(0)+} - \tau_{yx}^{(0)-})\right|_0 dx = 0 \\
&\int_{-\infty}^{\infty} \left.(\tau_{yy}^{(0)+} - \tau_{yy}^{(0)-})\right|_0 dx = 0
\end{aligned} \tag{32}$$

Since the boundary conditions are independent of x, we assume that

$$\psi_0 = f(y) \tag{36}$$

The most general solution of the biharmonic equation of the form given by equation (36) is

$$\psi_0^{\pm} = A^{\pm} y + B^{\pm} y^2 + C^{\pm} y^3 \tag{37}$$

Since terms proportional to y^3 give rise to external pressure gradients, these terms will be ignored in the stream functions. The kinematic boundary conditions give

$$A^{\pm} = 1$$

$$A^{\pm} \pm 2B^{\pm} h = 1 - V_{P0} \tag{38}$$

For the equilibrium boundary condition, we must find the stresses $\tau_{yx}^{(0)\pm}$, $\tau_{yy}^{(0)\pm}$ and the pressure $p_0^{\pm}$. From (35), we see that

$$\tau_{yy}^{(0)\pm} = -p_0^{\pm}$$

$$\tau_{yx}^{(0)\pm} = -2B^{\pm} \tag{39}$$

and

$$\frac{\partial p_0^{\pm}}{\partial x} = -\frac{\partial^3 \psi_0^{\pm}}{\partial x^2 \partial y} - \frac{\partial^3 \psi_0^{\pm}}{\partial y^3} = 0$$

$$\frac{\partial p_0^{\pm}}{\partial y} = \frac{\partial^3 \psi_0^{\pm}}{\partial x^3} + \frac{\partial^3 \psi_0}{\partial x \partial y^2} = 0$$

so that

$$p_0^{\pm} = \text{constant} = 0 \tag{40}$$

since we have assumed we have no imposed pressure gradients.

Substituting (39) and (40) into (32), we get

$$\int_{-\infty}^{\infty} (-2B^{+} + 2B^{-})\, dx = 0 \tag{41}$$

For this to be true, we find

$$-B_1^{+} + B^{-} = 0$$

and

$$B^{+} = B^{-}. \tag{42}$$

Solving (42) and (38) simultaneously leads to

$$A^{+} = A^{-} = 1$$

$$B^{+} = B^{-} = V_{P_0} = 0 \tag{43}$$

and

$$\psi_0^{\pm} = y. \tag{44}$$

Equation (43) indicates that to zeroth order there is no propulsive velocity.

Equations (43) and (39) show that all stresses corresponding to the ψ_0 solution are identically zero. This leads to simplified forms of the first and second order equilibrium conditions. These are:

$$\begin{aligned} &\int_{-\infty}^{\infty} (\tau_{yx}^{(1)+} - \tau_{yx}^{(1)-})\Big|_0 \, dx = 0 \\ &\int_{-\infty}^{\infty} (\tau_{yy}^{(1)+} - \tau_{yy}^{(1)-})\Big|_0 \, dx = 0 \end{aligned} \tag{45}$$

$$\begin{aligned} &\int_{-\infty}^{\infty} [(\tau_{yx}^{(2)+} - \tau_{yx}^{(2)-}) - \cos x \, (\tau_{xx}^{(1)+} - \tau_{xx}^{(1)-}) \\ &\qquad + \sin x \, \frac{\partial}{\partial y} (\tau_{yx}^{(1)+} - \tau_{yx}^{(1)-})]\Big|_0 \, dx = 0 \\ &\int_{-\infty}^{\infty} [(\tau_{yy}^{(2)+} - \tau_{yy}^{(2)-}) - \cos x \, (\tau_{xy}^{(1)+} - \tau_{xy}^{(1)-}) \\ &\qquad + \sin x \, \frac{\partial}{\partial y} (\tau_{yy}^{(1)+} - \tau_{yy}^{(1)-})]\Big|_0 \, dx = 0 \end{aligned} \tag{46}$$

Also the kinematic boundary conditions simplify to

$$\begin{aligned} &\frac{\partial \psi_1}{\partial y}^{\pm}\Big|_0 = 0 \\ &\frac{\partial \psi_1}{\partial x}^{\pm}\Big|_0 = -\cos x \\ &\frac{\partial \psi_1}{\partial y}^{\pm}\Big|_{\pm h} = -V_{p_1} \\ &\frac{\partial \psi_1}{\partial x}^{\pm}\Big|_{\pm h} = \mp \beta \, m \, \gamma \, (\tilde{F} \cos mx - \tilde{G} \sin mx) \end{aligned} \tag{47}$$

and

$$\left.\frac{\partial \psi_2^{\pm}}{\partial y}\right|_0 = -\left.\frac{\partial^2 \psi_1^{\pm}}{\partial y^2}\right|_0 \sin x$$

$$\left.\frac{\partial \psi_2^{\pm}}{\partial x}\right|_0 = -\left.\frac{\partial^2 \psi_1^{\pm}}{\partial x \partial y}\right|_0 \sin x$$

(48)

$$\left.\frac{\partial \psi_2^{\pm}}{\partial y}\right|_{\pm h} = -V_{p_2} \mp \beta \left.\frac{\partial^2 \psi_1^{\pm}}{\partial y^2}\right|_{\pm h} (\tilde{F} \sin mx + \tilde{G} \cos mx)$$

$$\left.\frac{\partial \psi_2^{\pm}}{\partial x}\right|_{\pm h} = \mp\beta \left.\frac{\partial^2 \psi_1^{\pm}}{\partial x \partial y}\right|_{\pm h} (\tilde{F} \sin mx + \tilde{G} \cos mx).$$

We now proceed to find a solution to equations (27), (45), and (47). Seeking a solution of the form

$$\begin{aligned}\psi_1^{\pm} = {} & [(A^{\pm} + B^{\pm} y) \sinh y + (C^{\pm} + D^{\pm} y \cosh y] \sin x \\ & + [(E^{\pm} + F^{\pm} y) \sinh my + (G^{\pm} + H^{\pm} y) \cosh my] \sin mx \\ & + [(I^{\pm} + J^{\pm} y) \sinh my + (K^{\pm} + L^{\pm} y) \cosh my] \cos mx \\ & + M^{\pm} y + N^{\pm} y^2,\end{aligned} \tag{49}$$

We assume that m is fractional or an integer. This assumption is necessary since we would like the sine and the cosine functions to be orthogonal. It is not a severe restriction on the generality of the solution, since if an interaction is to occur between the wall and sheet it should be present at or near an assumed value of m. Since the solution will be periodic with period $2n\pi$, the equilibrium condition (45) can also be expressed as

$$\int_{-\infty}^{\infty} [\ ]\, dx = 0 \Longrightarrow \int_0^{2n\pi} [\ ]\, dx = 0 \tag{50}$$

With the assumed form for $\psi_1^{\pm}$,(49), and the boundary conditions, (47) and (50), we find (see Appendix IV)

$$M^{\pm} = N^{\pm} = V_{p_1} = 0. \tag{51}$$

ψ_1 now takes the form

$$\begin{aligned}\psi_1^{\pm} = & - [\cosh y \pm d(\sinh y - y \cosh y) + e\, y \sinh y] \sin x \\ & - \beta\gamma\ (\tilde{F} \sin mx + \tilde{G} \cos mx) \\ & [f\ (\sinh my - my \cosh my) \pm g\, my \sinh my]\end{aligned} \tag{52}$$

where

$$\begin{aligned} d &= -[\cosh(h)\ \sinh(h)+h]/[\sinh^2(h) - h^2] \\ e &= -\ \sinh^2(h)/[\sinh^2(h) - h^2] \\ f &= [mh \cosh(mh) + \sinh(mh)]/[\sinh^2(mh) - m^2h^2] \\ g &= mh\ \sinh(mh)/[\sinh^2(mh) - m^2h^2] \end{aligned} \tag{53}$$

The propulsive velocity is zero to first order.

Since the governing equation (27) for $\psi_2^{\pm}$ is the same as $\psi_0^{\pm}$ and $\psi_1^{\pm}$, we may find the propulsive velocity by assuming a form for $\psi_2^{\pm}$ which satisfies equation (27) and by using only the

$$\left.\frac{\partial \psi_2^{\pm}}{\partial y}\right|_{0,\pm h}$$

and force boundary conditions. The kinematic boundary conditions are

$$\left.\frac{\partial \psi_2}{\partial y}^{\pm}\right|_0 = -\left.\frac{\partial^2 \psi_1}{\partial y^2}^{\pm}\right|_0 \sin x$$

$$\left.\frac{\partial \psi_2}{\partial y}^{\pm}\right|_{\pm h} = -V_p \mp \beta \left.\frac{\partial^2 \psi_1}{\partial y^2}\right|_{\pm h} (\tilde{F} \sin mx + \tilde{G} \cos mx) \tag{54}$$

These boundary conditions (54) become (see Appendix V)

$$\left.\frac{\partial \psi_2}{\partial y}^{\pm}\right|_0 = -\frac{\ell}{2} + \frac{\ell}{2} \cos 2x$$

$$\pm\beta\gamma\, m^2 g \{\tilde{F}[\cos(m-1)\, x - \cos(m+1)x]$$

$$+ \tilde{G}[\sin(m+1)\, x - \sin(m-1)x]\}$$

$$\left.\frac{\partial \psi_2}{\partial y}^{\pm}\right|_{\pm h} = -V_{p_2} - \beta^2\gamma m^2 \frac{\ell^*}{2} \pm \beta\, q \{\tilde{F}[\cos(m-1)\, x - \cos(m+1)\, x] \tag{55}$$

$$+ \tilde{G}[\sin(m+1)\, x - \sin(m-1)\, x]\}$$

$$- \beta^2\gamma\, m^2 \frac{\ell^*}{2} [2\tilde{F}\, \tilde{G} \sin 2mx + (\tilde{G}^2 - \tilde{F}^2) \cos 2mx]$$

where

$$\ell = [\sinh^2(h) + h^2]/[\sinh^2(h) - h^2]$$

$$\ell^* = [\sinh^2(mh) + m^2h^2]/[\sinh^2(mh) - m^2h^2]$$

$$q = h \sinh(h)/[\sinh^2(h) - h^2].$$

We now assume that $\psi_2^{\pm}$ satisfies the governing equation

$$\nabla^4 \psi_2^{\pm} = 0 \tag{27}$$

and has, like $\psi_0^{\pm}$ and $\psi_1^{\pm}$, the following form

$$\psi_2^{\pm} = \text{sine terms} + \text{cosine terms} + M^{\pm} y + N^{\pm} y^2. \qquad (56)$$

Then the differentiation of (56) and evaluation at $y = 0, \pm h$ give the following equations for $M^{\pm}$ and $N^{\pm}$ when matched with the constant terms in (55)

$$\begin{aligned} M^{\pm} &= -\frac{\ell}{2} \\ M^{\pm} \pm 2N^{\pm} h &= V_{p2} - \beta^2 \gamma m^2 \frac{\ell}{2}^* \end{aligned} \qquad (57)$$

From the force equilibrium condition (see Appendix VI), we find

$$N^+ = N^- . \qquad (58)$$

Solving (57) and (58) and rewriting our results in dimensional form yields,

$$\begin{aligned} V_p &= c_s b_s^2 k_s^2 \frac{\ell}{2} - c_w b_w^2 k_w^2 \frac{\ell}{2}^* \\ N^+ &= N^- = 0 \end{aligned} \qquad (59)$$

This gives a second order propulsive velocity for the sheet which is affected by the wall oscillation.

In equation (59), the propulsive velocity is found to be composed of two parts. The first portion of the velocity is identical to Reynolds (1965) result. The second is found to be the same as the velocity of a free (i.e., no net force acting) flat sheet being pumped in a channel. The total sheet velocity to order α^2 is the sum of these two problems as indicated in Fig. II-9.

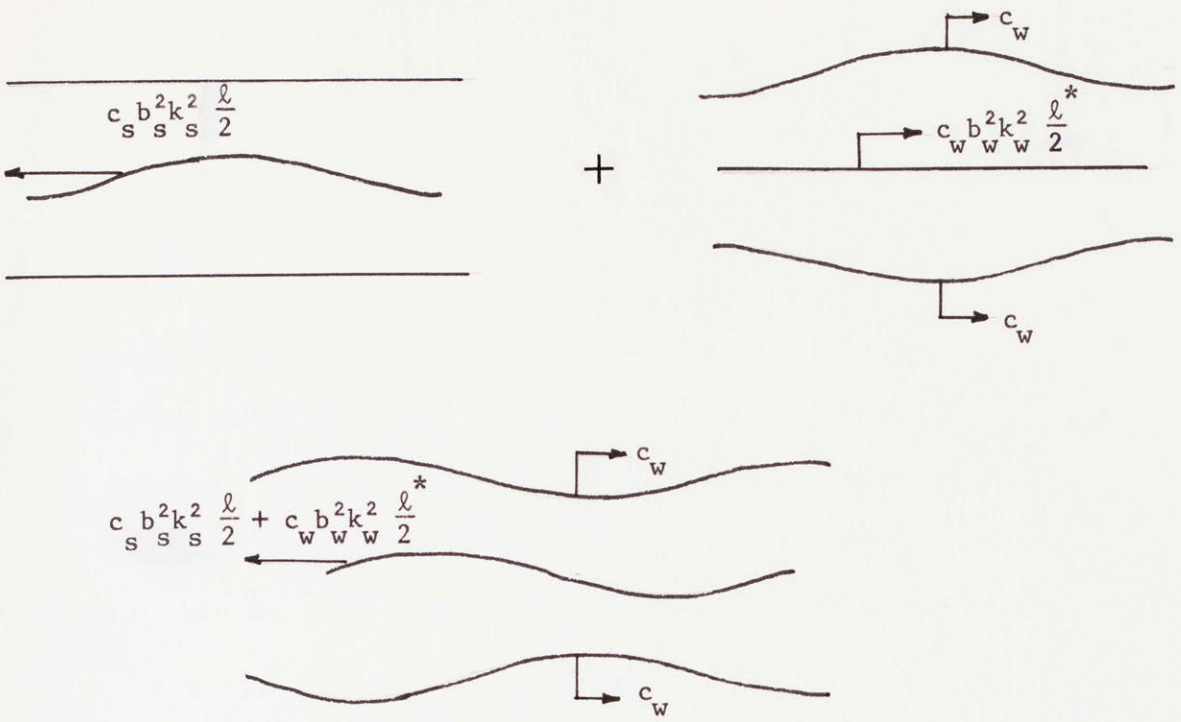

Fig. II-9

It is also interesting to look at some limiting cases of equation (59). As the amplitude of the wall motion goes to zero, the result becomes

$$b_w \to 0 \qquad V_p = c_s b_s^2 k_s^2 \frac{\ell}{2} \tag{60}$$

which is Reynolds' (1965) result as expected. For the walls going to infinity, we find

$$h \to \infty \qquad V_p = \frac{1}{2} c_s b_s^2 k_s^2 - \frac{1}{2} c_w b_w^2 k_w^2 \tag{61}$$

which shows that the effect of the active boundary at infinity is felt throughout the fluid.

Another special case of interest is that of equal wavelengths of the sheet and wall. For m = 1, equation (59) can be written

$$V_p = c_s\, b_s^2\, k_s^2\, \frac{\ell}{2}\, (1 - \beta^2\gamma). \tag{62}$$

Equation (62) indicates that for a wave traveling in the same direction as the sheet wave, the velocity will always be less than Reynolds' (1965) result.

Although equation (59) gives V_p as a function of bk, $k_s h$ and $k_w h$, it is difficult to determine the wall effect on propulsion unless the energy output of the sheet is fixed. To compute the rate of energy dissipation, we must relate the stream function and velocities in Frame 3 to the corresponding quantities in the stationary Frame 1. The total power dissipated is

$$W = -\int_{y_s} (\underset{\sim}{T}^+ \cdot \underset{\sim}{u}^+) + (\underset{\sim}{T}^- \cdot \underset{\sim}{u}^-)\, ds \tag{63}$$

where $\underset{\sim}{u}^{\pm}$ are velocities in the fixed frame.

The power expenditure per wavelength in dimensionless form is (see Appendix VII)

$$W = -2d + O(\alpha^3). \tag{64}$$

This expression for the energy is identical to that of Reynolds (1965) and is sketched in Fig. II-3. This result is simply the rate at which work is being done by the sheet against the first order pressure terms.

A final quantity of interest is the flow rate through the channel. This is given by

$$Q = \int_{y_w}^{y_s} u^-\, dy + \int_{y_s}^{y_w^+} u^+\, dy \tag{65}$$

which in terms of the stream function is

$$Q = -\int_{y_w}^{y_s} \frac{\partial \psi^-}{\partial y}\, dy - \int_{y_s}^{y_w^+} \frac{\partial \psi^+}{\partial y}\, dy \tag{66}$$

where $u^{\pm}$ and $\psi^{\pm}$ are calculated in the fixed frame. Integrating (66) we find

$$Q = \psi^{+}(y_s) + \psi^{-}(y_w^{-}) - [\psi^{+}(y_w^{+}) + \psi^{-}(y_s)] \tag{67}$$

The average flow rate over a period is (see Appendix VII)

$$\overline{Q} = h\,\alpha^2\,\beta^2 m^2\,\gamma\,\ell^* + O(\alpha^3) \tag{68}$$

or in dimensional form to second order

$$\overline{Q} = h\,b_w^2\,k_w^2\,c_w\,\ell^* \tag{69}$$

The flow is seen to be produced only by the motion of the wall.

A similar analysis can be carried out for the case of a left traveling wave and a standing wave. The results are presented in Table III-1, and details of the calculation are found in Appendices A-VIII and A-IX.

Section III: Results and Discussion

Table III-1 summarizes the results of the present investigation in dimensional form.

Wall Shape	Propulsive Velocity in Terms of Geometry	Propulsive Velocity in Terms of Energy Expended
Flat Wall (Reynolds)	$b_s^2 k_s^2 c_s \frac{\ell}{2}$	$\frac{W}{2\mu k_s c_s^2 d}\left(c_s \frac{\ell}{2}\right)$
Standing Wave	$b_s^2 k_s^2 c_s \frac{\ell}{2}$	$\frac{W}{2\mu k_s c_s^2 d}\left(c_s \frac{\ell}{2}\right)$
Traveling Wave		
Right	$b_s^2 k_s^2 c_s \frac{\ell}{2} - b_w^2 k_w^2 c_w \frac{\ell^*}{2}$	$\frac{W}{2\mu k_s c_s^2 d}\left[c_s \frac{\ell}{2} + \left(\frac{b_w k_w}{b_s k_s}\right)^2 c_w \frac{\ell^*}{2}\right]$
Left	$b_s^2 k_s^2 c_s \frac{\ell}{2} + b_w^2 k_w^2 c_w \frac{\ell^*}{2}$	$\frac{W}{2\mu k_s c_s^2 d}\left[c_s \frac{\ell}{2} - \left(\frac{b_w k_w}{b_s k_s}\right)^2 c_w \frac{\ell^*}{2}\right]$

$$\ell = \frac{\sinh^2(k_s h) + k_s^2 h^2}{\sinh^2(k_s h) - k_s^2 h^2} \qquad W = -2b_s^2 k_s^3 \mu c_s^2 d \qquad \ell^* = \frac{\sinh^2(k_w h) + k_w^2 h^2}{\sinh^2(k_w h) - k_w^2 h^2}$$

$$d = \frac{\cosh(k_s h)\sinh(k_s h) + k_s h}{\sinh^2(k_s h) - k_s^2 h^2}$$

Table III-1

Before presenting a discussion of these results, it is interesting to note that the solution to the present problem clarifies some aspects of Reynolds' (1965) treatment of the sheet between two fixed walls.

In obtaining the solution to this problem, it was necessary to seek the stream function in both the region above and below the sheet. This was required since the sheet was to have no net viscous force acting on it. In Reynolds' (1965) paper, the solution in both regions was not considered for the sheet moving at mid-channel. Only the kinematic boundary conditions on the sheet and on the walls were imposed on the solution. This led to questions concerning the uniqueness of his solution. These difficulties do not arise if the force boundary conditions on the sheet are considered. To complete the formulation of the problem the imposed pressures at the ends of the channel must be specified. The kinematic boundary conditions together with the force condition and a statement concerning imposed pressures give a unique solution to the posed problem.

From Table III-1, for the case of the traveling waves, we see that the velocity is composed of two terms. The first is a term involving only the motion of the sheet. The second term involves only the motion of the wall. The problem (to the order considered) can be shown to be the superposition of Reynolds' (1965) problem and that of a rigid flat sheet being pumped in a channel (see Fig. II-9). For waves passing in the direction of motion of the sheet, the velocity is increased by the wall action, while for waves moving in a direction opposite the sheet motion, the velocity is decreased. For the right and left traveling wave, it should be noted that the propulsive velocity can be written for equal wavelengths as

$$V_p = \frac{\ell}{2} [b_s^2 k^2 c_s \mp b_w^2 k^2 c_w]$$

where $k = k_s$.

In this form, we see that the velocity increases or decreases linearly with the phase velocity of the waves and quadratically with the amplitudes.

In the case of standing waves on the wall the propulsive velocity is the same as Reynolds'(1965) result for fixed walls. Again to second order, standing waves can be thought of as the superposition of two traveling waves in opposite directions (see Appendix IX). The energy expenditure for movement in a channel as sketched in Fig. II-3, is greater than that in an infinite media for equal amplitudes of oscillation. This increased energy expenditure does lead to increased velocities of propulsion. However, the rapid rate of energy dissipation is not consistent with a physically realistic situation.

The velocity for a fixed energy expenditure is given in Fig. II-4. This velocity is seen to increase by only 10% at the optimal channel spacing, $k_s h$, equal to 2. No "resonance" interaction exists between the sheet and the vibrating walls.

These results are inconsistent with Odeblad's (1962) hypothesis that sperm move with greatly increased velocity and minimum energy expenditures, between the vibrating micelles, i.e., between channels with standing waves.

In view of the present work, it seems that Odeblad's (1962) theory of enhanced propulsive sperm velocity by vibrating walls is not supported by a detailed analysis of an analogous low Reynolds number flow problem.

Alternatives do exist, however, which may explain enhanced transport in the cervix. On the basis of the data in Table I-2, the time required for sperm to pass through the cervix on its own motility (25mm, Carlborg, 1969)

is approximately 15 minutes. This estimate for the transit time is not unreasonable based on the observations of Rubenstein, et.al., that sperm are present in the Fallopian tubes 30 minutes after deposition on the cervix (Davajan, et.al., 1970).

Though Odeblad's "resonance" and "minimum energy" theory could not be demonstrated the cervix may still possibly be assigned an "active" role in sperm transport. These "active" functions may be due to alignment of sperm, biochemical enhancement or "insuck". The micellular structure of cervical mucus which Odeblad has presented offers one explanation for the speed with which sperm move through the cervix. (Odeblad's estimates of 5μ/sec for the velocity of sperm are below those of other investigators in Table I-2.) The micelles form channels which may guide the sperm. This causes the sperm to move directly toward the uterus and not randomly or diffusely in the mucus.

Observations on the effect of pH in increasing swimming speed have been noted previously. It has also been noted that the low viscosity component of cervical mucus contains nutrients necessary for the metabolic processes of the sperm. Mann observed (Moghissi and Blandau, 1972) that the sperm could utilize aerobic metabolism in the cervix which is a much more efficient method of obtaining energy than the anaerobic metabolism of the sperm in the male tract.

The theory of "insuck" has, perhaps, been too quickly dismissed (Sobrero, 1963; Sobrero and MacCleod, 1962) as a method of transport of sperm. The measurements of Fox, Wolff and Baker (1970) on the drop of intrauterine pressure should be given more careful attention. The pressure drop observed during orgasm is not small and the duration is on the order of minutes. Under these conditions, it is possible that retrograde flow could occur in the

cervix as observed by Enhorning, et.al. (1963), and aid in sperm transport.

The present work has presented a survey of the function of the cervix in sperm transport. It has also sought to verify aspects of a theory of sperm transport through the cervix proposed by Odeblad (1962). Based on the analysis of a simple model this theory does not seem supportable. Other "active" roles may be assigned to the cervix, however, The structure of cervical mucus presented by Odeblad offers a method by which the sperm may pass directly through the cervix. Aspects of biochemical enhancement of motility and "insuck" also offer possible mechanisms for accelerated transport and should be further investigated. The mechanism of sperm transport is biologically complex and not yet know.

"Finally . . . the only statement that can be made with absolute certainty is that spermatozoa do get into the upper genital tract." (Davajan, et.al., 1970).

References

Belonoschkin, B. 1960. "The Problem of Cervical Biology", Int'l. J. Fertil., 5, 38-43.

Bergman, P. 1953. "Spermigration and Cyclic Changes in Cervical Mucus", Fertil. & Steril., 4, 183-193.

Bibliography on Sperm Transport Through the Cervix in Mammals. 1970. Reproduction Research Information Service Ltd., Cambridge, England.

Blandau, R.J. 1969. "Gamete Transport-Comparative Aspects", in The Mammalian Oviduct, Comparative Biology and Methodology, Hafez, E.S.E. & Blandau, R.J., eds., Univ. of Chicago Press, Chicago, 129-162.

Carlborg, Lars. 1969. "Determination of Sperm Migration Rate in Small Samples of Cervical Mucus", Acta Endoc., 62, 732-746.

Davajan, V., Nakamura, R.M., and Kharma, K. 1970. "Spermatozoan Transport in Cervical Mucus", Obstetrics & Gynec. Survey, 25, 1-43.

Davajan, V., Nakamura, R.M., and Mishell, D.R. 1971. "A Simplified Technique for Evaluation of the Biophysical Properties of Cervical Mucus", Am. J. Obstet. & Gynec., 109, 1042-1048.

deBoer, C.H. 1972. "Transport of Particulate Matter through the Human Female Genital Tract", J. Reprod. Fert. 28, 295-297.

Drummond, J.E. 1966. "Propulsion by Oscillating Sheets and Tubes in a Viscous Fluid", J. Fluid Mech., 25, 787-793.

Egli, G.E. and Newton, M. 1961. "The Transport of Carbon Particles in the Human Female Reproductive Tract", Fert. & Steril., 12, 151-155.

Elstein, M. and MacDonald, R.R. 1970. "The Relation of Cervical Mucus Proteins to Sperm Penetrability", J. Obstet. Gynec. Br. Comm., 77, 1123-1126.

Elstein, M., Mitchell, R.F., and Syrett, J.T. 1971. "Ultrastructure of Cervical Mucus", J. Obstet. Gynec. Br. Comm., 78, 180-183.

Enhorning, G., Ingelman-Sundberg, A. and Joelsson, I. 1963. "Recording Flow through the Cervical Canal", Fertil. & Steril., 14, 494-499.

Fox, C.A. and Fox, B. 1967. "Uterine Suction During Orgasm", Br. Med. J., 1, 300-301.

Fox, C.A. and Fox, B. 1969. "Blood Pressure and Respiratory Patterns during Human Coitus", J. Reprod. Fertil., 19, 405-415.

Fox, C.A., Wolff, H.S. and Baker, J.A. 1970. "Measurement of Intra-vaginal and Intra-uterine Pressures during Human Coitus by Radio-Telemetry", J. Reprod. Fertil., 22, 243-251.

Gibbons, R.A. and Mattner, P. 1966. "Some Aspects of the Chemistry of Cervical Mucus", Int'l. J. Fert., 11, 366.

Gibbons, R.A. and Mattner, P. 1971. "The Chemical and Physical Characteristics of the Cervical Secretion and Its Role in Reproductive Physiology", in Pathways to Conception, Sherman, A.I., ed., Chas. C. Thomas, Springfield, Ill., 143-155.

Gray, J., and Hancock, G.J. 1955. "The Propulsion of Sea-urchin Spermatozoa", J. Exp. Biol., 32, 802-814.

Hafez, E.S.E. and Kanagawa, H. 1971. "Cervical Epithelium and Spermatozoa", Exhibit, VII World Con gress of Fert. & Sterl, Tokyo, Japan.

Hafez, E.S.E., Kanagawa, H., Meynet, A., and Jaszczak, S. 1972. Physiology of Reproduction Film Series, Sperm Transport and Cilia Activity in the Cervix of the Rabbit, (booklet), Depts. of Gynec.-Obstet. and Physiology, Wayne State Univ., Detroit, Mich.

Hancock, G.J. 1953. "The Self-Propulsion of Microscopic Organisms through Liquids", Proc. Roy. Soc. Lond., A217, 96-121.

Harvey, C. 1960. "The Speed of Human Spermatozoa and the Effect on It of Various Diluents, with some preliminary Observations on Clinical Material", J. Reprod. Fertil., 1, 84-95.

Illingsworth, C.R. 1963. "Flow at Small Reynolds Numbers", in Laminar Boundary Layers, Rosenhead, L., ed., Oxford Univ. Press, 163.

Karni, Z., Polishuk, W.Z. Adoni, A., and Diamant, Y. 1971. "Newtonian Viscosity of the Human Cervical Mucus during the Menstrual Cycle", Int'l. J. Fertil., 16, 185-188.

MacDonald, R.R. and Lumley, I.B. 1970. "Endocervical pH Measured in Vivo through the Normal Menstrual Cycle", Obstet. & Gynec., 35, 202-206.

Marcus, C.C. and Marcus, S.L. 1968. "The Cervical Factor", in Progress in Infertility, Behrman, S.J. and Kistner, R.W., eds., Little, Brown and Co., Boston, 21-62.

Moghissi, K.S. 1966. "Cyclic Changes of Cervical Mucus in Normal and Progestin-Treated Women", Fertil. & Ster., 17, 663-675.

Moghissi, K.S. 1968. "Human and Bovine Sperm Migration", Fertil. & Steril., 19, 118-122.

Moghissi, K.S. 1969. "Sperm Migration in the Human Female Genital Tract", J. Reprod. Med. 3, 73-85.

Moghissi, K.S. 1971. "Sperm Migration Through Cervical Mucus", in Pathways to Conception, Sherman, A., ed., Chas. C. Thomas, Springfield, Ill., 214-236.

Moghissi, K.S. 1972. "The Function of the Cervix in Fertility", Fertil. & Steril., 23, 295-306.

Moghissi, K.S. and Blandau, R.J. 1972. "Biology of the Cervix, Summary of a Symposium held at Lake Wilderness, Washington, June 9-12, 1971", J. Reprod. Med., 8, 21-25.

Moghissi, K.S., Dabich, D., Levine, J., and Neuhaus, O.W. 1964. "The Mechanism of Sperm Migration", Fertil. & Steril., 15, 15-23.

Moghissi, K.S. and Syner, F.N. 1970. "Studies on Human Cervical Mucus: Mucoids and their Relation to Sperm Penetration", Fertil. & Steril., 21, 234-239.

Odeblad, E. 1959. "The Physics of the Cervical Mucus", Acta Obstet. & Gynec. Scand., 38, (Supp. 1), 44-58.

Odeblad, E. 1962. "Undulations of Macromolecules in Cervical Mucus", Int'l. J. of Fertil., 7, 313-319.

Odeblad, E. 1966. "Micro-NMR in High Permanent Magnetic Fields", Acta Obstet. & Gynec. Scand., 45, (Supp. 2).

Odeblad, E. 1968. "The Functional Structure of Cervical Mucus", Acta Obstet. & Gynec. Scand., 47, (Supp. 1), 59-79.

Odeblad, E. 1969. "Types of Human Cervical Secretion", Acta Europ. Fertil., 1, 99-116.

Odeblad, E. 1971. "Cervical Factors", Nobel Symposium 15, Control of Human Fertility, Diczfalusy, E. and Borell, U., eds., John Wiley & Sons, Inc., 89-96.

Odeblad, E. and Rosenberg, B. 1968. "A Low Viscosity Component in Human Uterine Endocervical Contents", Acta. Obstet. & Gynec. Scand., 47, 345-349.

Reynolds, A.J. 1965. "The Swimming of Minute Organisms", J. Fluid Mech., 23, 241-260.

Schumacher, G.F.B. 1970. "Biochemistry of Cervical Mucus", Fertil. & Steril., 21, 697-705.

Sobrero, A.J. 1963. "Sperm Migration in the Female Genital Tract", in Mechanisms Concerned with Conception, Hartman, C.G., ed., MacMillian, 173-204.

Sobrero, A.J. 1967. "Sperm Migration in the Human Female", Proc. 5th World Cong. on Fertil. & Steril., Stockholm, Westin, B. & Wiquist, N., eds., Exerpta Medka Fnd., 701-703.

Sobrero, A.J. 1969. "The Cervical Factor in Human Infertility", World Health Organization, Scientific Group on Basic, Clinical and Public Health Aspects of Subfertility and Sterility.

Sobrero, A.J. and MacLeod, J. 1962. "The Immediate Postcoital Test", Fertil. & Steril., 13, 184-189.

Tampion, D., and Gibbons, R.A. 1962. "Orientation of Spermatozoa in Mucus of the Cervix Uteri", Nature, 194, 381.

Taylor, G.I. 1951. "Analysis of the Swimming of Microscopic Organisms", Proc. Roy. Soc. Lond., A209, 447-461.

Taylor, G.I. 1952. "The Action of Waving Cylindrical Tails in Propelling Microscopic Organisms", Proc. Roy. Soc. Lond., A211, 225-239.

Tuck, E.O. 1968. "A Note on a Swimming Problem", J. Fluid Mech., 31, 305-308.

Appendix I

Analysis of Swimming Sheet in an Infinite Medium

Taylor (1951) analyzed a doubly infinite sheet swimming in an unbounded medium. The sheet was assumed to have the form as given by

$$y = b \sin k(x - ct) \tag{AI-1}$$

relative to an observer fixed on the sheet, Frame 2, (Fig. AI-1).

Fig. AI-1

For an observer moving with a velocity c, Frame 3, the sheet appears to be a fixed curve. The velocity and coordinate transformations are

$$\begin{aligned} u_2 &= u_3 + c \quad , \quad x_2 = x_3 + ct \\ v_2 &= v_3 \quad , \quad y_2 = y_3 \end{aligned} \tag{AI-2}$$

Applying (AI-2) to (AI-1), we find

$$y_3 = b \sin k x_3 \tag{AI-3}$$

Now in Frame 3 the particles on the sheet are seen to slide along the curve (AI-3) with a velocity Q.

Taylor (1951) then assumed the sheet to be inextensible. For the inextensible sheet, a particle will move with a constant velocity which is

always tangent to the curve, Fig. AI-2,

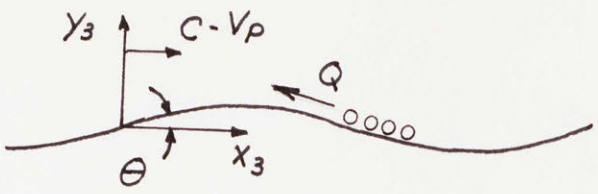

Fig. AI-2

The velocities of the particles relative to Frame 3 are given by

$$u_3 = -Q\cos\theta \quad , \quad v_3 = -Q\sin\theta \tag{AI-4}$$

where

$$\tan\theta = \frac{dy_3}{dx_3} \tag{AI-5}$$

The quantity Q is yet to be determined.

To determine Q, we note that for a periodic motion, Frame 2, a particle at point x_2 will return to x_2 in one period, T. Then from (AI-2), we find

$$x_3(t) + ct = x_3(t+T) + c(t+T) \tag{AI-6}$$

or

$$x_3(t) - x_3(t+T) = cT = \lambda \tag{AI-7}$$

which represents the distance traveled by the particle, as seen by the moving observer. So the particle moves one arc length in a period and

$$Q = \frac{\text{ARC LENGTH}}{T} = \frac{c}{\lambda}\int_0^{\lambda}\frac{ds}{dx_3}\,dx_3 = \frac{c}{\lambda}\int_0^{\lambda}\sqrt{1+\left(\frac{dy_3}{dx_3}\right)^2}\,dx_3 \tag{AI-8}$$

For the form of the sheet (AI-3), Q equals

$$Q = \frac{c}{2\pi} \int_0^{2\pi} \sqrt{1 + b^2 k^2 \cos^2 x_3}\, dx_3 \qquad \text{(AI-9)}$$

Expanding (AI-9), in powers of bk and integrating

$$Q = c \left[1 + \frac{1}{4} b^2 k^2 + O(b^4 k^4) \right] \qquad \text{(AI-10)}$$

Using (AI-10) with (AI-4) and (AI-5), we find by expanding the trigonometric functions in series

$$u_3 = -c \left[1 - \frac{1}{4} b^2 k^2 \cos 2kx + O(b^4 k^4) \right]$$
$$v_3 = -c \left[bk \cos kx + O(b^3 k^3) \right] \qquad \text{(AI-11)}$$

The boundary conditions at infinity for Frame 3 are given by

$$u_\infty = V_p - c$$
$$v_\infty = 0 \qquad \text{(AI-12)}$$

The governing partial differential equation in terms of the stream function is

$$\nabla^4 \psi = 0 \qquad \text{(AI-13)}$$

where

$$u = -\frac{\partial \psi}{\partial y}, \quad v = \frac{\partial \psi}{\partial x}$$

A solution can be sought in terms of an asymptotic series as outlined in

Equations (20), (24), and (25). The result of such an expansion is the following governing equations and boundary conditions (terms involving ψ_0 have been omitted from ψ_1 and ψ_2).

$$\nabla^4 \psi_0 = 0$$

$$\left.\frac{\partial \psi_0}{\partial y}\right|_0 = c \quad , \quad \lim_{y\to\infty} \frac{\partial \psi_0}{\partial y} = c - V_{P_0}$$

$$\left.\frac{\partial \psi_0}{\partial x}\right|_0 = 0 \quad , \quad \lim_{y\to\infty} \frac{\partial \psi_0}{\partial x} = 0 \qquad \text{(AI-14)}$$

$$\nabla^4 \psi_1 = 0$$

$$\left.\frac{\partial \psi_1}{\partial y}\right|_0 = 0 \quad , \quad \lim_{y\to\infty} \frac{\partial \psi_1}{\partial y} = -V_{P_1}$$

$$\left.\frac{\partial \psi_1}{\partial x}\right|_0 = -c\cos kx \quad , \quad \lim_{y\to\infty} \frac{\partial \psi_1}{\partial x} = 0 \qquad \text{(AI-15)}$$

$$\nabla^4 \psi_2 = 0$$

$$\left.\frac{\partial \psi_2}{\partial y}\right|_0 = -\frac{c}{4}\cos 2kx - \left.\frac{\partial^2 \psi_1}{\partial y^2}\right|_0 \frac{1}{k}\sin kx$$

$$\left.\frac{\partial \psi_2}{\partial x}\right|_0 = -\left.\frac{\partial^2 \psi_1}{\partial x \partial y}\right|_0 \frac{1}{k}\sin kx$$

$$\lim_{y\to\infty} \frac{\partial \psi_2}{\partial y} = -V_{P_2} \qquad \text{(AI-16)}$$

$$\lim_{y\to\infty} \frac{\partial \psi_2}{\partial x} = 0$$

The solution to (AI-19) to (AI-16) to second order is found to be

$$V_p = c\,\frac{b^2k^2}{2} \qquad \text{(AI-17)}$$

We may investigate how the swimming speed is affected by the properties of the sheet by assuming the sheet to be "peristaltic" in nature. In contrast to the inextensible sheet, adjacent particles on a "peristaltic" sheet move independently. This means, that in a frame where the motion of the sheet is simple periodic motion, the horizontal and vertical velocities are

$$u = 0\ , \qquad v = \frac{\partial y}{\partial t} \qquad \text{(AI-18)}$$

In Frame 2, the motion is seen to be periodic. Using (AI-1), we find from (AI-18)

$$u_2 = 0\ , \quad v_2 = -\,c\,b\,k\,\cos k(x_2 - ct) \qquad \text{(AI-19)}$$

Moving to Frame 3, the velocities are

$$u_3 = -c\ , \quad v_3 = -\,c\,b\,k\,\cos k x_3 \qquad \text{(AI-20)}$$

The boundary conditions at infinity are again (AI-12) and after expanding as previously indicated,we find the following equations corresponding to (AI-14) through (AI-16)

$$\nabla^4 \psi_0 = 0$$

$$\left.\frac{\partial \psi_0}{\partial y}\right|_0 = c \;, \quad \lim_{y \to \infty} \frac{\partial \psi_0}{\partial y} = c - V_{P_0}$$

$$\left.\frac{\partial \psi_0}{\partial x}\right|_0 = 0 \;, \quad \lim_{y \to \infty} \frac{\partial \psi_0}{\partial x} = 0 \qquad \text{(AI-21)}$$

$$\nabla^4 \psi_1 = 0$$

$$\left.\frac{\partial \psi_1}{\partial y}\right|_0 = 0$$

$$\left.\frac{\partial \psi_1}{\partial x}\right|_0 = -c \cos kx$$

$$\lim_{y \to \infty} \frac{\partial \psi_1}{\partial y} = -V_{P_1} \qquad \text{(AI-22)}$$

$$\lim_{y \to \infty} \frac{\partial \psi_1}{\partial x} = 0$$

$$\nabla^4 \psi_2 = 0$$

$$\left.\frac{\partial \psi_2}{\partial y}\right|_0 = -\left.\frac{\partial^2 \psi_1}{\partial y^2}\right|_0 \frac{1}{k} \sin kx$$

$$\left.\frac{\partial \psi_2}{\partial x}\right|_0 = -\left.\frac{\partial^2 \psi_1}{\partial x \, \partial y}\right|_0 \frac{1}{k} \sin kx \qquad \text{(AI-23)}$$

$$\lim_{y \to \infty} \frac{\partial \psi_2}{\partial y} = -V_{P_2}$$

$$\lim_{y \to \infty} \frac{\partial \psi_2}{\partial x} = 0$$

The solution to (AI-21) to (AI-23) is found to be

$$V_p = c\,\frac{b^2k^2}{2} \qquad \text{(AI-24)}$$

This result agrees with the previous result of Taylor (1951). This correspondence between peristaltic and inextensible sheets was observed by Tuck (1968) in a discussion of Reynolds' results. Of course, when higher order terms are considered, the propulsion velocity will depend on the nature of the sheet.

Appendix II

Expansion of the Force Boundary Condition

The equilibrium statement given by equation (19) is

$$\int_{\gamma_s} (\underset{\sim}{T}^{+} + \underset{\sim}{T}^{-})\, ds = 0$$

The evaluation of this integral requires the forces to be known on the sheet. In order to evaluate the integral, the forces will be represented in terms of the stress tensor which will be expanded in a Taylor series about the mean plane of the sheet. Since it is convenient in this development, indicial notation and the summation convention will be used. Rewriting (19) in this manner gives

$$\int_{\gamma_s} (T_i^{+} + T_i^{-})\, ds = 0 \qquad i = 1, 2 \tag{AII-1}$$

where

$$T_i^{\pm} = n_j^{\pm}\, \tau_{ji}^{\pm} \tag{AII-2}$$

and

n_j = unit outward normal to the sheet

τ_{ij} = stress tensor

Let the unit normal and the stress tensor be represented by

$$\begin{aligned} n_j^{\pm} &= n_j^{(0)\pm} + \alpha\, n_j^{(1)\pm} + \alpha^2 n_j^{(2)\pm} + O(\alpha^3) \\ \tau_{ji}^{\pm} &= \tau_{ji}^{(0)\pm} + \alpha\, \tau_{ji}^{(1)\pm} + \alpha^2 \tau_{ji}^{(2)\pm} + O(\alpha^3) \end{aligned} \tag{AII-3}$$

Substituting (AII-3) into (AII-2), we obtain

$$T_i^{\pm} = n_j^{(0)\pm}\,\tilde{\tau}_{ji}^{(0)\pm} + \alpha\left(n_j^{(0)\pm}\,\tilde{\tau}_{ji}^{(1)\pm} + n_j^{(1)\pm}\,\tilde{\tau}_{ji}^{(0)\pm}\right) + \alpha^2\left(n_j^{(0)\pm}\,\tilde{\tau}_{ji}^{(2)\pm} + n_j^{(1)\pm}\,\tilde{\tau}_{ji}^{(1)\pm} + n_j^{(2)\pm}\,\tilde{\tau}_{ji}^{(0)\pm}\right) + O(\alpha^3) \qquad \text{(AII-4)}$$

Expanding $\tilde{\tau}_{ji}^{(n)\pm}$ in a Taylor series about y = 0, gives

$$\tilde{\tau}_{ji}^{(n)\pm} = \tilde{\tau}_{ji}^{(n)\pm}\Big|_0 + \frac{\partial}{\partial x_2}\,\tilde{\tau}_{ji}^{(n)\pm}\Big|_0 x_{2s} + \frac{1}{2}\,\frac{\partial^2}{\partial x_2}\,\tilde{\tau}_{ji}^{(n)\pm}\Big|_0 x_{2s}^2 + \cdots \qquad \text{(AII-5)}$$

where

$$x_{2s} = \alpha \sin x_1$$

Substitution into (AII-4) yields,

$$T_i^{\pm} = n_j^{(0)\pm}\,\tilde{\tau}_{ji}^{(0)\pm}\Big|_0 + \alpha\left(n_j^{(0)\pm}\tilde{\tau}_{ji}^{(1)\pm} + n_j^{(1)\pm}\,\tilde{\tau}_{ji}^{(0)\pm} + n_j^{(0)\pm}\frac{\partial}{\partial x_2}\,\tilde{\tau}_{ji}^{(0)\pm}\sin x_1\right)\Big|_0 + \alpha^2\left(n_j^{(0)\pm}\tilde{\tau}_{ji}^{(2)\pm} + n_j^{(1)\pm}\,\tilde{\tau}_{ji}^{(1)\pm} + n_j^{(2)\pm}\,\tilde{\tau}_{ji}^{(0)\pm} + \frac{1}{2}n_j^{(0)\pm}\frac{\partial^2}{\partial x_2^2}\,\tilde{\tau}_{ji}^{(0)}\sin^2 x_1 + n_j^{(0)\pm}\frac{\partial}{\partial x_2}\,\tilde{\tau}_{ji}^{(1)\pm}\sin x_1 + n_j^{(1)\pm}\frac{\partial}{\partial x_2}\,\tilde{\tau}_{ji}^{(0)\pm}\sin x_1\right)\Big|_0 \qquad \text{(AII-6)}$$

From Appendix III, the components of the normal are

$$n_j^{(0)} = (0, 1)$$
$$n_j^{(1)} = (-\cos X_1, 0) \qquad \text{(AII-7)}$$
$$n_j^{(2)} = (0, -\tfrac{1}{2}\cos^2 X_1)$$

and noting that $n_j^{(n)+} = -n_j^{(n)-}$, equation (AII-6) can be written

$$\begin{aligned} T_i^+ + T_i^- = {} & (\tau_{2i}^{(0)+} - \tau_{2i}^{(0)-})\big|_0 \\ & + \alpha\left[(\tau_{2i}^{(1)+} - \tau_{2i}^{(1)-}) - \cos X_1 (\tau_{1i}^{(0)+} - \tau_{1i}^{(0)-})\right. \\ & \quad \left. + \sin X_1 \frac{\partial}{\partial X_2}(\tau_{2i}^{(0)+} - \tau_{2i}^{(0)-})\right]\Big|_0 \\ & + \alpha^2\left[(\tau_{2i}^{(2)+} - \tau_{2i}^{(2)-}) - \cos X_1 (\tau_{1i}^{(1)+} - \tau_{1i}^{(1)-})\right. \\ & \quad - \tfrac{1}{2}\cos^2 X_1 (\tau_{2i}^{(0)+} - \tau_{2i}^{(0)-}) \\ & \quad + \tfrac{1}{2}\sin^2 X_1 \frac{\partial^2}{\partial X_2^2}(\tau_{2i}^{(0)+} - \tau_{2i}^{(0)-}) \\ & \quad + \sin X_1 \frac{\partial}{\partial X_2}(\tau_{2i}^{(1)+} - \tau_{2i}^{(1)-}) \\ & \quad \left. - \sin X_1 \cos X_1 \frac{\partial}{\partial X_2}(\tau_{1i}^{(0)+} - \tau_{1i}^{(0)-})\right]\Big|_0 \end{aligned} \qquad \text{(AII-8)}$$

where 1 and 2 denote x and y directions respectively. Now the arc length may be represented by

$$ds = dX_1\sqrt{1+\left(\frac{dX_2}{dX_1}\right)^2} = dX_1\sqrt{1+\alpha^2\cos^2 X_1}$$
$$ds = dX_1\left[1 + \tfrac{1}{2}\alpha^2\cos^2 X_1 + O(\alpha^4)\right] \qquad \text{(AII-9)}$$

Using (AII-8) and (AII-9) the equilibrium expression (AII-1) becomes

$$\int_{-\infty}^{\infty} \left(\tilde{\tau}_{2i}^{(0)+} - \tilde{\tau}_{2i}^{(0)-} \right) dx_1$$

$$+ \alpha \int_{-\infty}^{\infty} \left[\left(\tilde{\tau}_{2i}^{(1)+} - \tilde{\tau}_{2i}^{(1)-} \right) - \cos x_1 \left(\tilde{\tau}_{1i}^{(0)+} - \tilde{\tau}_{1i}^{(0)-} \right) \right.$$

$$\left. + \sin x_1 \frac{\partial}{\partial x_2} \left(\tilde{\tau}_{2i}^{(0)+} - \tilde{\tau}_{2i}^{(0)-} \right) \right]\Big|_0 dx_1$$

$$+ \alpha^2 \int_{-\infty}^{\infty} \left[\left(\tilde{\tau}_{2i}^{(2)+} - \tilde{\tau}_{2i}^{(2)-} \right) - \cos x_1 \left(\tilde{\tau}_{1i}^{(1)+} - \tilde{\tau}_{1i}^{(1)-} \right) \right.$$

$$+ \frac{1}{2} \sin^2 x_1 \frac{\partial^2}{\partial x_2^2} \left(\tilde{\tau}_{2i}^{(0)+} - \tilde{\tau}_{2i}^{(0)-} \right) \qquad \text{(AII-10)}$$

$$+ \sin x_1 \frac{\partial}{\partial x_2} \left(\tilde{\tau}_{2i}^{(1)+} + \tilde{\tau}_{2i}^{(1)-} \right)$$

$$\left. - \sin x_1 \cos x_1 \left(\tilde{\tau}_{1i}^{(0)+} - \tilde{\tau}_{1i}^{(0)-} \right) \right]\Big|_0 dx_1 + O(\alpha^3) = 0$$

$$i = 1, 2$$

Equation (AII-10) is the desired expression for the force boundary conditions.

Appendix III

Computation of the Outward Normal to the Sheet

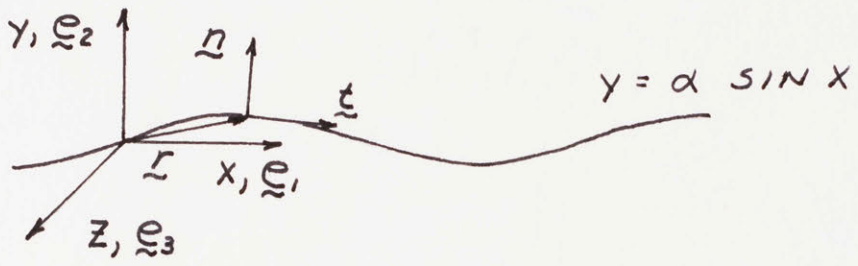

Fig. AIII-1

The outward normal vector (Fig. AIII-1) to the sheet is equal to

$$\underset{\sim}{n} = \underset{\sim}{e}_3 \times \underset{\sim}{t} \tag{AIII-1}$$

The tangent vector $\underset{\sim}{t}$ is defined by

$$\underset{\sim}{t} = \frac{d\underset{\sim}{r}}{ds} \tag{AIII-2}$$

where

$$\underset{\sim}{r} = x\,\underset{\sim}{e}_1 + y\,\underset{\sim}{e}_2 \tag{AIII-3}$$

Substituting (AIII-3) into (AIII-2), we obtain

$$\underset{\sim}{t} = \frac{dx}{ds}\left(\underset{\sim}{e}_1 + \frac{dy}{dx}\,\underset{\sim}{e}_2\right) \tag{AIII-4}$$

Now

$$ds^2 = dx^2\left[1 + \left(\frac{dy}{dx}\right)^2\right] \tag{AIII-5}$$

from which we obtain

$$\frac{dx}{ds} = \left[1 + \left(\frac{dy}{dx}\right)^2 \right]^{-1/2} \qquad \text{(AIII-6)}$$

Combining (AIII-6) with (AIII-4) we find

$$\underset{\sim}{t} = \left[1 + \left(\frac{dy}{dx}\right)^2 \right]^{-1/2} \left(\underset{\sim}{e}_1 + \frac{dy}{dx} \underset{\sim}{e}_2 \right) \qquad \text{(AIII-7)}$$

but,

$$y = \alpha \sin x \qquad \text{(AIII-8)}$$

and

$$\frac{dy}{dx} = \alpha \cos x \qquad \text{(AIII-9)}$$

Substituting (AIII-9) into (AIII-7) and expanding, we obtain

$$\underset{\sim}{t} = \left[1 - \tfrac{1}{2} \alpha^2 \cos^2 x + O(\alpha^4) \right] \left(\underset{\sim}{e}_1 + \alpha \cos x \, \underset{\sim}{e}_2 \right) \qquad \text{(AIII-10)}$$

Finally, we find from (AIII-1)

$$\underset{\sim}{n} = \left[-\alpha \cos x + O(\alpha^3) \right] \underset{\sim}{e}_1 + \left[1 - \tfrac{1}{2} \alpha^2 \cos^2 x + O(\alpha^4) \right] \underset{\sim}{e}_2$$

the outward normal to the sheet.

Appendix IV

Determination of the First Order Stream Function

The assumed form of the stream function given by (49) is

$$\psi_1^{\pm} = [(A^{\pm} + B^{\pm}y)\sinh y + (C^{\pm} + D^{\pm}y)\cosh y]\sin x$$
$$+ [(E^{\pm} + F^{\pm}y)\sinh my + (G^{\pm} + H^{\pm}y)\cosh my]\sin mx$$
$$+ [(I^{\pm} + J^{\pm}y)\sinh my + (K^{\pm} + L^{\pm}y)\cosh my]\cos mx \qquad \text{(AIV-1)}$$

Differentiating (AIV-1) with respect to x and y and evaluating at y = 0, $\pm$h boundary conditions, (47), become

$$\left.\frac{\partial \psi_1^{\pm}}{\partial y}\right|_0 = (A^{\pm} + D^{\pm}) \sin x + (m E^{\pm} + H^{\pm}) \sin mx + (m I^{\pm} + L^{\pm}) \cos mx + M^{\pm} = 0$$

$$\left.\frac{\partial \psi_1^{\pm}}{\partial x}\right|_0 = C^{\pm} \cos x + m G^{\pm} \cos mx - m K^{\pm} \sin mx = -\cos x$$

(AIV-2)

$$\begin{aligned}\left.\frac{\partial \psi_1^{\pm}}{\partial y}\right|_{\pm h} = {} & [(A^{\pm} \pm B^{\pm} h) \cosh(h) \pm B^{\pm} \sinh(h) \\ & \pm (C^{\pm} \pm D^{\pm} h) \sinh(h) + D^{\pm} \cosh(h)] \sin x \\ & + [m(E^{\pm} \pm F^{\pm} h) \cosh(mh) \pm F^{\pm} \sinh(mh) \\ & \pm m(G^{\pm} \pm H^{\pm} h) \sinh(mh) + H^{\pm} \cosh(mh)] \sin mx \\ & + [m(I^{\pm} \pm J^{\pm} h) \cosh(mh) \pm J^{\pm} \sinh(mh) \\ & \pm m(K^{\pm} \pm L^{\pm} h) \sinh(mh) + L^{\pm} \cosh(mh)] \sin mx \\ & + M^{\pm} \pm 2N^{\pm} h = -V_{p_1}\end{aligned}$$

$$\begin{aligned}\left.\frac{\partial \psi_1^{\pm}}{\partial x}\right|_{\pm h} = {} & [\pm(A^{\pm} \pm B^{\pm} h) \sinh(h) + (C^{\pm} \pm D^{\pm} h) \cosh(h)] \sin x \\ & + m[\pm(E^{\pm} \pm F^{\pm} h) \sinh(mh) + (G^{\pm} \pm H^{\pm} h) \cosh(mh)] \cos mx \\ & - m[\pm(I^{\pm} \pm J^{\pm} h) \sinh(mh) + (K^{\pm} \pm L^{\pm} h) \cosh(mh)] \sin mx \\ & = \mp \beta m Y [\tilde{F} \cos mx - \tilde{G} \sin mx]\end{aligned}$$

Since m is considered to be an integer or fraction, the sine and cosine terms are orthogonal over a properly chosen period, and equations (AIV-2) give rise to the following sets of simultaneous equations,

$$A^{\pm} \pm D^{\pm} = 0$$

$$C^{\pm} = -1 \qquad \text{(AIV-3)}$$

$$(A^{\pm} \pm B^{\pm}h)\cosh(h) \pm B^{\pm}\sinh(h) \pm (C^{\pm} \pm D^{\pm}h)\sinh(h) + D^{\pm}\cosh(h) = 0$$

$$\pm(A^{\pm} \pm B^{\pm}h)\sinh(h) + (C^{\pm} \pm D^{\pm}h)\cosh(h) = 0$$

$$mE^{\pm} + H^{\pm} = 0$$

$$mG^{\pm} = 0$$

$$m(E^{\pm} \pm F^{\pm}h)\cosh(mh) \pm F^{\pm}\sinh(mh) \qquad \text{(AIV-4)}$$
$$\pm m(G^{\pm} \pm H^{\pm}h)\sinh(mh) + H^{\pm}\cosh(mh) = 0$$

$$m[\pm(E^{\pm} \pm F^{\pm}h)\sinh(mh) + (G^{\pm} \pm H^{\pm}h)\cosh(mh)] = \mp\beta\gamma m\tilde{F}$$

$$mI^{\pm} + J^{\pm} = 0$$

$$mK^{\pm} = 0$$

$$m(I^{\pm} \pm J^{\pm}h)\cosh(mh) \pm J^{\pm}\sinh(mh) \qquad \text{(AIV-5)}$$
$$\pm m(K^{\pm} \pm L^{\pm}h)\sinh(mh) + H^{\pm}\cosh(mh) = 0$$

$$m[\pm(I^{\pm} \pm J^{\pm}h)\sinh(mh) + (K^{\pm} \pm L^{\pm}h)\cosh(mh)] = \mp\beta\gamma m\tilde{G}$$

$$M^{\pm} = 0 \qquad \text{(AIV-6)}$$

$$M^{\pm} \pm 2N^{\pm}h = -V_{p_1}$$

From (AIV-6), we see that

$$\pm 2N^{\pm} h = -V_{p_1} \qquad \text{(AIV-7)}$$

V_{p_1} and $N^{\pm}$ must be determined from the force equilibrium condition. Before proceeding, we solve (AIV-3) to (AIV-5) and find that,

$$A^{\pm} = -D^{\pm} = \pm \frac{\cosh(h)\sinh(h) + h}{\sinh^2(h) - h^2}$$

$$B^{\pm} = \frac{\sinh^2(h)}{\sinh^2(h) - h^2}$$

$$C^{\pm} = -1$$

$$H^{\pm} = -m E^{\pm} = \frac{\beta\gamma m \tilde{F}\left[mh\cosh(mh) + \sinh(mh)\right]}{\sinh^2(mh) - m^2h^2}$$

$$F^{\pm} = \mp \frac{\gamma m^2 \beta \tilde{F} h \sinh(mh)}{\sinh^2(mh) - m^2h^2} \qquad \text{(AIV-8)}$$

$$L^{\pm} = -m I^{\pm} = \frac{\beta\gamma m \tilde{G}\left[mh\cosh(mh) + \sinh(mh)\right]}{\sinh^2(mh) - m^2h^2}$$

$$J^{\pm} = \mp \frac{\gamma m^2 \beta \tilde{G} h \sinh(mh)}{\sinh^2(mh) - m^2h^2}$$

$$G^{\pm} = K^{\pm} = 0$$

With equations (AIV-8) and (AIV-6), the stream function becomes,

$$\psi_1^{\pm} = -[\cosh y \pm d(\sinh y - y\cosh y) + e\, y \sinh y]\sin x - \beta\gamma(\tilde{F}\sin mx + \tilde{G}\cos mx)[f(\sinh my - my\cosh my) \pm g\, my \sinh my] + N \pm y^2 \quad \text{(AIV-9)}$$

where

$$d = -\frac{\cosh(h)\sinh(h) + h}{\sinh^2(h) - h^2}$$

$$e = -\frac{\sinh^2(h)}{\sinh^2(h) - h^2} \quad \text{(AIV-10)}$$

$$f = \frac{mh\cosh(mh) + \sinh(mh)}{\sinh^2(mh) - m^2h^2}$$

$$g = \frac{mh\sinh(mh)}{\sinh^2(mh) - m^2h^2}$$

To find $N^{\pm}$ and V_{p_1}, we must use the force equilibrium condition equation (50)

$$\int_0^{2n\pi} [\ ]\, dx = 0 \qquad \text{(AIV-11)}$$

This, for the first order solution, is (45)

$$\int_0^{2n\pi} (\tau_{yx}^{(1)+} - \tau_{yx}^{(1)-})|_0\, dx = 0$$
$$\int_0^{2n\pi} (\tau_{yy}^{(1)+} - \tau_{yy}^{(1)-})|_0\, dx = 0 \qquad \text{(AIV-12)}$$

where

$$\tau_{yx}^{(1)\pm}|_0 = \left(-\frac{\partial^2 \psi_1^{\pm}}{\partial y^2} + \frac{\partial^2 \psi_1^{\pm}}{\partial x^2}\right)|_0$$
$$\tau_{yy}^{(1)\pm}|_0 = \left(-p_1^{\pm} + 2\frac{\partial^2 \psi_1^{\pm}}{\partial x\, \partial y}\right)|_0 \qquad \text{(AIV-13)}$$

$$\frac{\partial p_1^{\pm}}{\partial x} = -\frac{\partial^3 \psi_1^{\pm}}{\partial x^2 \partial y} - \frac{\partial^3 \psi_1^{\pm}}{\partial y^3} \qquad \text{(a)}$$

$$\frac{\partial p_1^{\pm}}{\partial y} = \frac{\partial^3 \psi_1^{\pm}}{\partial x^3} + \frac{\partial^3 \psi_1^{\pm}}{\partial y^2 \partial x} \qquad \text{(b)}$$

From (AIV-9), we find

$$\frac{\partial^2 \psi_1^{\pm}}{\partial y^2} = -[\cosh y \mp d(\sinh y + y\cosh y) + e(2\cosh y + y\sinh y)]\sin x + \beta\gamma m^2(\tilde{F}\sin mx + \tilde{G}\cos mx)[f(\sinh my + my\cosh my) \mp g(2\cosh my + my\sinh my)] + 2N^{\pm}$$

$$\frac{\partial^2 \psi_1^{\pm}}{\partial x^2} = [\cosh y \pm d(\sinh y - y\cosh y) + e\, y\sinh y]\sin x + \beta\gamma m^2(\tilde{F}\sin mx + \tilde{G}\cos mx)[f(\sinh my - my\cosh my) \pm g\, my\sinh my] \quad \text{(AIV-14)}$$

$$\frac{\partial^2 \psi_1^{\pm}}{\partial x \partial y} = -[\sinh y \mp d\, y\sinh y + e(\sinh y + y\cosh y)]\cos x + \beta\gamma m^2(\tilde{F}\cos mx - \tilde{G}\sin mx)[f\, my\sinh my \mp g(\sinh my + my\cosh my)]$$

The pressure gradient is given by

$$\frac{\partial p_1^{\pm}}{\partial x} = -\left(\frac{\partial^3 \psi_1^{\pm}}{\partial x^2 \partial y} + \frac{\partial^3 \psi_1^{\pm}}{\partial y^3} \right) \qquad \text{(AIV-15)}$$

or

$$p_1^{\pm} = -\int \left(\frac{\partial^3 \psi_1^{\pm}}{\partial x^2 \partial y} + \frac{\partial^3 \psi_1^{\pm}}{\partial y^3} \right) dx + f(y) \qquad \text{(AIV-16)}$$

From (AIV-13b), we find f(y) equals a constant, which must be zero since we have assumed no imposed pressure gradient. Then, the expression for $p_1^{\pm}$ becomes

$$p_1^{\pm} = -\frac{\partial^2 \psi_1^{\pm}}{\partial x \partial y} - \int \frac{\partial^3 \psi_1^{\pm}}{\partial y^3} dx \qquad \text{(AIV-17)}$$

From (AIV-14), differentiating $\frac{\partial^2 \psi_1^{\pm}}{\partial y^2}$ with respect to y gives

$$\begin{aligned} \frac{\partial^3 \psi_1^{\pm}}{\partial y^3} = -[& \sinh y \mp d(2\cosh y + y \sinh y) \\ & + e(3 \sinh y + y \cosh y)] \sin x \\ & + \beta \gamma m^3 (\tilde{F} \sin mx + \tilde{G} \cos mx) \\ & [f(2 \cosh my + my \sinh my) \\ & \mp g(3 \sinh my + my \cosh my)] \end{aligned} \qquad \text{(AIV-18)}$$

The pressure then becomes, from (AIV-18) and (AIV-14)

$$p_1^{\pm} = -\left[\mp 2d \cosh y + 2e \sinh y\right] \cos x + \beta\gamma m^2 \left(\tilde{F} \cos mx - \tilde{G} \sin mx\right) \left[2f \cosh my \mp 2g \sinh my\right] \tag{AIV-19}$$

From (AIV-14) and (AIV-19), (AIV-13) becomes

$$\tau_{yx}^{(1)\pm}\Big|_0 = (1+2e) \sin x - 2N^{\pm} + \sin x \pm 2\beta\gamma m^2 g \left(\tilde{F} \sin mx + \tilde{G} \cos mx\right) \tag{AIV-20}$$

$$\tau_{yy}^{(1)\pm}\Big|_0 = \mp 2d \cos x - 2\beta\gamma m^2 f \left(\tilde{F} \sin mx + \tilde{G} \cos mx\right)$$

and the force boundary condition becomes, upon substitution of (AIV-20) into (AIV-12)

$$\int_0^{2n\pi} \left[4\beta\gamma m^2 g \left(\tilde{F} \sin mx + \tilde{G} \cos mx\right) - 2N^+ + 2N^-\right] dx = 0 \tag{AIV-21}$$

$$\int_0^{2n\pi} -4d \cos x \, dx = 0$$

These equations are satisfied if

$$N^+ = N^- \tag{AIV-22}$$

Now with (AIV-22), we find from (AIV-7) that

$$V_{P1} = 0 \tag{AIV-23}$$

and

$$N^{+} = N^{-} = 0 \tag{AIV-24}$$

Thus the propulsive velocity and shear flow vanish to this order.

Appendix V

Calculation of Second Order Kinematic Boundary Conditions

The boundary conditions (54) are

$$\left.\frac{\partial \psi_2^{\pm}}{\partial y}\right|_0 = -\left.\frac{\partial^2 \psi_1^{\pm}}{\partial y^2}\right|_0 \sin x$$

$$\left.\frac{\partial \psi_2^{\pm}}{\partial y}\right|_{\pm h} = -V p_2 \mp \beta \left.\frac{\partial^2 \psi_1^{\pm}}{\partial y^2}\right|_{\pm h} (\tilde{F} \sin mx + \tilde{G} \cos mx) \tag{AV-1}$$

From Appendix IV, equation (AIV-14), we find $\frac{\partial^2 \psi_1^{\pm}}{\partial y^2}$. These derivatives evaluated at the designated limits are

$$\left.\frac{\partial^2 \psi_1^{\pm}}{\partial y^2}\right|_0 = -(1+2e)\sin x \mp 2\beta\gamma m^2 g (\tilde{F} \sin mx + \tilde{G} \cos mx) \tag{AV-2}$$

and

$$\left.\frac{\partial^2 \psi_1^{\pm}}{\partial y^2}\right|_{\pm h} = -\{\cosh(h) - d[\sinh(h) + h\cosh(h)] + e[2\cosh(h) + h\sinh(h)]\}\sin x + \beta\gamma m^2 (\tilde{F} \sin mx + \tilde{G} \cos mx) \tag{AV-3}$$

$$\{\pm f[\sinh(mh) + mh\cosh(mh)] \mp g[2\cosh(mh) + mh\sinh(mh)]\}$$

From (AIV-10) we substitute the definition of d, e, f, and g, and find

$$\ell = -[1+2e] = \frac{\sinh^2(h) + h^2}{\sinh^2(h) - h^2}$$

$$2g = \{\cosh(h) - d[\sinh(h) + h\cosh(h)] + e[2\cosh(h) + h\sinh(h)]\}$$

$$= \frac{2h\sinh(h)}{\sinh^2(h) - h^2} \qquad \text{(AV-4)}$$

$$\pm \ell^* = \pm f[\sinh(mh) + mh\cosh(mh)] \mp g[2\cosh(mh) + mh\sinh(mh)]$$

$$= \pm \frac{\sinh^2(mh) + m^2h^2}{\sinh^2(mh) - m^2h^2}$$

Substituting (AV-4) into (AV-3) and then into (AV-1), the boundary conditions are

$$\left.\frac{\partial \psi_2^{\pm}}{\partial y}\right|_0 = -\ell \sin^2 x \pm 2\beta\gamma m^2 g \left(\tilde{F} \sin mx + \tilde{G} \cos mx\right) \sin x$$

$$\left.\frac{\partial \psi_2^{\pm}}{\partial y}\right|_{\pm h} = -V_{p2} \pm \beta \left[2g \sin x \mp \beta\gamma m^2 \ell^* \left(\tilde{F} \sin mx + \tilde{G} \cos mx\right)\right]\left(\tilde{F} \sin mx + \tilde{G} \cos mx\right) \qquad \text{(AV-5)}$$

Expanding the trigonometric functions and performing the multiplications, we get

$$\left.\frac{\partial \psi_2^{\pm}}{\partial y}\right|_0 = -\frac{\ell}{2} + \frac{\ell}{2} \cos 2x \pm \beta\gamma m^2 g \left\{\tilde{F}\left[\cos(m-1)x - \cos(m+1)x\right] + \tilde{G}\left[\sin(m+1)x - \sin(m-1)x\right]\right\}$$

$$\left.\frac{\partial \psi_2^{\pm}}{\partial y}\right|_{\pm h} = -V_{p2} - \beta^2\gamma m^2 \frac{\ell^*}{2} \pm \beta g \left\{\tilde{F}\left[\cos(m-1)x - \cos(m+1)x\right] + \tilde{G}\left[\sin(m+1)x - \sin(m-1)x\right]\right\} - \beta^2\gamma m^2 \frac{\ell^*}{2}\left[2\tilde{F}\tilde{G} \sin 2mx + (\tilde{G}^2 - \tilde{F}^2) \cos 2mx\right] \qquad \text{(AV-6)}$$

which are the desired boundary conditions.

Appendix VI

Determination of the Second Order Equilibrium Condition

The equilibrium equation for the second order solution is given by (46) and with equation (50) becomes

$$\int_0^{2n\pi} \left[\left(\tau_{yx}^{(2)+} - \tau_{yx}^{(2)-} \right) - \cos x \left(\tau_{xx}^{(1)+} - \tau_{xx}^{(1)-} \right) + \sin x \frac{\partial}{\partial y} \left(\tau_{yx}^{(1)+} - \tau_{yx}^{(1)-} \right) \right]_0 dx = 0$$

$$\int_0^{2n\pi} \left[\left(\tau_{yy}^{(2)+} - \tau_{yy}^{(2)-} \right) - \cos x \left(\tau_{xy}^{(1)+} - \tau_{xy}^{(1)-} \right) + \sin x \frac{\partial}{\partial y} \left(\tau_{yy}^{(1)+} - \tau_{yy}^{(1)-} \right) \right]_0 dx = 0 \qquad \text{(AVI-1)}$$

The stresses are given by (35). Rewriting them for reference we have

$$\begin{aligned} \tau_{xx}^{(n)\pm} &= -p_n^{\pm} - 2 \frac{\partial^2 \psi_n^{\pm}}{\partial x \partial y} \\ \tau_{yy}^{(n)\pm} &= -p_n^{\pm} + 2 \frac{\partial^2 \psi_n^{\pm}}{\partial x \partial y} \\ \tau_{xy}^{(n)\pm} &= -\frac{\partial^2 \psi_n^{\pm}}{\partial y^2} + \frac{\partial^2 \psi_n^{\pm}}{\partial x^2} \end{aligned} \qquad \text{(AVI-2)}$$

and

$$\frac{\partial p_n^{\pm}}{\partial x} = -\frac{\partial^3 \psi_n^{\pm}}{\partial x^2 \partial y} - \frac{\partial^3 \psi_n^{\pm}}{\partial y^3} \qquad \text{(a)}$$

$$\frac{\partial p_n^{\pm}}{\partial y} = \frac{\partial^3 \psi_n^{\pm}}{\partial x^3} + \frac{\partial^3 \psi_n^{\pm}}{\partial y^2 \partial x} \qquad \text{(b)}$$

From the assumed form for $\psi_2^{\pm}$ (56)

$$\psi_2^{\pm} = \text{SINE TERMS} + \text{COSINE TERMS} + M^{\pm} y + N^{\pm} y^2 \qquad \text{(AVI-3)}$$

we see that

$$\tilde{\tau}_{xy}^{(2)\pm} = \text{SINE TERMS} + \text{COSINE TERMS} - 2N^{\pm} \qquad \text{(AVI-4)}$$

The pressure is found from (AVI-2a) by integration;

$$\frac{\partial p_2^{\pm}}{\partial x} = -\frac{\partial^3 \psi_2^{\pm}}{\partial x^2 \partial y} + \frac{\partial^3 \psi_2^{\pm}}{\partial y^3}$$

$$= \text{SINE TERMS} + \text{COSINE TERMS} \qquad \text{(AVI-5)}$$

$$p_2^{\pm} = \text{SINE TERMS} + \text{COSINE TERMS} + f(y)$$

From (AVI-2b) we find f(y) equals a constant which must be zero since we have assumed no imposed pressure gradients. Then from (AVI-5), (AVI-3), and (AVI-2), we find

$$\tilde{\tau}_{yy}^{(2)\pm} = \text{SINE TERMS} + \text{COSINE TERMS} \qquad \text{(AVI-6)}$$

For the $\tilde{\tau}^{(1)\pm}$ terms, we have from Appendix IV, (AIV-19),

$$p_1^{\pm} = -[\mp 2d \cosh y + 2e \sinh y] \cos x + \beta\gamma m^2 (\tilde{F} \cos mx - \tilde{G} \sin mx) [2f \cosh my \mp 2g \sinh my] \quad \text{(AVI-7)}$$

and (AIV-14)

$$\frac{\partial^2 \psi_1^{\pm}}{\partial x \partial y} = -[\sinh y \mp d\, y \sinh y + e(\sinh y + y \cosh y)] \cos x + \beta\gamma m^2 (\tilde{F} \cos mx - \tilde{G} \sin mx) [f my \sinh my \mp g(\sinh my + my \cosh my)] \quad \text{(AVI-8)}$$

Then from (AVI-2), (AVI-7), and (AVI-8), we find

$$\tau_{xx}^{(1)\pm}|_0 = \mp 2d \cos x - 2\beta\gamma m^2 f (\tilde{F} \cos mx - \tilde{G} \sin mx) \quad \text{(AVI-9)}$$

and from Appendix IV (AIV-20, with $N^{\pm} = 0$)

$$\tau_{yx}^{(1)\pm}\Big|_0 = (1+2e)\sin x + \sin x \pm 2\beta\gamma m^2 g(\bar{F}\sin mx + \tilde{G}\cos mx) \qquad \text{(AVI-10)}$$

From (AVI-2), we find,

$$\frac{\partial \tau_{yy}^{(1)\pm}}{\partial y} = -\frac{\partial p^{\pm}}{\partial y} + 2\frac{\partial^3 \psi_1^{\pm}}{\partial x \partial y^2} \qquad \text{(AVI-11)}$$

and

$$\frac{\partial \tau_{xy}^{(1)\pm}}{\partial y} = -\frac{\partial^3 \psi_1^{\pm}}{\partial y^3} + \frac{\partial^3 \psi_1^{\pm}}{\partial x^2 \partial y} \qquad \text{(AVI-12)}$$

Differentiating (AVI-7) and (AVI-8), yields

$$\frac{\partial p_1^{\pm}}{\partial y} = -(\mp 2d\sinh y + 2e\cosh y)\cos x + \beta\gamma m^3(\bar{F}\cos mx - \tilde{G}\sin mx)[2f\sinh my \mp 2g\cosh my] \qquad \text{(AVI-13)}$$

$$\frac{\partial^3 \psi_1^{\pm}}{\partial x \partial y^2} = -[\cosh y \mp d(\sinh y + y \cosh y) + e(2\cosh y + y \sinh y)] \cos x + \beta\gamma m^3 (\tilde{F} \cos mx - \tilde{G} \sin mx) \quad \text{(AVI-14)}$$
$$[f(\sinh my + my \cosh my \mp g(2\cosh my + my \sinh my)]$$

$$\frac{\partial^3 \psi_1^{\pm}}{\partial x^2 \partial y} = [\sinh y \mp d\, y \sinh y + e(\sinh y + y \cosh y)] \sin x - \beta\gamma m^3 (\tilde{F} \sin mx + \tilde{G} \cos mx) \quad \text{(AVI-15)}$$
$$[f\, my \sinh my \mp g(\sinh my + my \cosh my)]$$

and from (AIV-18)

$$\frac{\partial^3 \psi_1^{\pm}}{\partial y^3} = -[\sinh y \mp d(2\cosh y + y \sinh y) + e(3\sinh y + y \cosh y)] \sin x + \beta\gamma m^3 (\tilde{F} \sin mx + \tilde{G} \cos mx) \quad \text{(AVI-16)}$$
$$[f(2\cosh my + my \sinh my) \mp g(3\sinh my + my \cosh my)]$$

Substitution of (AVI-13) to (AVI-16) into (AVI-11) and (AVI-12) gives on evaluation at y = 0,

$$\left.\frac{\partial \tau_{yy}^{(1)\pm}}{\partial y}\right|_0 = -2(1+e)\cos x \mp 2\beta\gamma m^3 g(\tilde{F}\cos mx - \tilde{G}\sin mx) \qquad \text{(AVI-17)}$$

$$\left.\frac{\partial \tau_{xy}^{(1)\pm}}{\partial y}\right|_0 = \mp 2d\sin x - 2\beta\gamma m^3 f(\tilde{F}\sin mx + \tilde{G}\cos mx) \qquad \text{(AVI-18)}$$

with (AVI-4), (AVI-6), (AVI-9), (AVI-10), (AVI-17), and (AVI-18), equations (AVI-1) become

$$\int_0^{2n\pi} [(\text{SINE TERMS} + \text{COSINE TERMS} - 2N^+ + 2N^-) + 4d\cos^2 x - 4d\sin^2 x]\,dx = 0 \qquad \text{(AVI-19)}$$

$$\int_0^{2n\pi} [(\text{SINE TERMS} + \text{COSINE TERMS}) - 4\beta\gamma m^2 g(\tilde{F}\sin mx + \tilde{G}\cos mx)\cos x - 4\beta\gamma m^3 g(\tilde{F}\cos mx - \tilde{G}\sin mx)\sin x]\,dx = 0$$

Carrying out the integration, we obtain

$$+2d - 2d - 4n\pi N^+ + 4n\pi N^- = 0 \qquad \text{(AVI-20)}$$

and

$$N^+ = N^- \qquad \text{(AVI-21)}$$

This is the equation required to determine V_{p2}.

For the case m = 1, (AVI-19) gives

$$+2d - 2d - 4n\pi N^+ + 4n\pi N^- = 0$$

$$-2\beta\gamma g + 2\beta\gamma g = 0 \qquad \text{(AVI-22)}$$

and again

$$N^+ = N^- \qquad \text{(AVI-23)}$$

Appendix VII

Calculation of Energy Expended and Flow Rate

The energy dissipated per wavelength by the sheet in the fixed frame is given by (64)

$$W = -\int_0^{\lambda} (\underset{\sim}{T}^{+} \cdot \underset{\sim}{u}^{+}) + (\underset{\sim}{T}^{-} \cdot \underset{\sim}{u}^{-})\, ds \qquad \text{(AVII-1)}$$

The velocity and coordinates in the fixed Frame, 1, are related to Frame 3 by the following transformations

$$u_1^{\pm} = u_3^{\pm} + 1 - V_p \quad , \quad x_1 = x_3 + (1 - V_p)t$$

$$V_1^{\pm} = V_3^{\pm} \quad , \quad y_1 = y_3 \qquad \text{(AVII-2)}$$

From the stream function, we find

$$u_3^{\pm} = -\left[\frac{\partial \psi_0^{\pm}}{\partial y} + \alpha \frac{\partial \psi_1^{\pm}}{\partial y} + \alpha^2 \frac{\partial \psi_2^{\pm}}{\partial y} + O(\alpha^3) \right] \qquad \text{(AVII-3)}$$

The velocity in the fixed frame is found by combining (AVII-3) and (AVII-2)

$$u_1^{\pm} = -\left[\frac{\partial \psi_0^{\pm}}{\partial y} + \alpha \frac{\partial \psi_1^{\pm}}{\partial y} + \alpha^2 \frac{\partial \psi_2^{\pm}}{\partial y} + O(\alpha^3) \right] + 1 - V_p \qquad \text{(AVII-4)}$$

Since

$$\psi_0^{\pm} = y_1$$

we find

$$u_1^{\pm} = -\left[\alpha \frac{\partial \psi_1^{\pm}}{\partial y} + \alpha^2 \left(\frac{\partial \psi_2^{\pm}}{\partial y} + V_{p_2} \right) + O(\alpha^3) \right] \qquad \text{(AVII-5)}$$

This indicates $u_1^{\pm}$ and $\psi^{\pm}$, the fixed frame velocity and stream functions, are $0(\alpha)$.

From the above and the expansion of $\underset{\sim}{T}$ in Appendix II (AII-10), we find the energy to be a second order quantity and equals

$$W = -\alpha^2 \int_0^{2n\pi} [(\tau_{yx}^{(1)+} - \tau_{yx}^{(1)-}) u_1 + (\tau_{yy}^{(1)+} - \tau_{yy}^{(1)-}) v_1]|_0 \, dx + O(\alpha^3) \qquad \text{(AVII-6)}$$

From the boundary condition (47), we see that

$$u_1|_0 = 0 \qquad \text{(AVII-7)}$$

and (AVII-6) reduces to

$$W = -\alpha^2 \int_0^{2n\pi} [(\tau_{yy}^{(1)+} \tau_{yy}^{(1)-}) v_1]|_0 \, dx + O(\alpha^3) \qquad \text{(AVII-8)}$$

Equation (AIV-20) gives

$$(\tau_{yy}^{(1)+} - \tau_{yy}^{(1)-})|_0 = -4d \cos[x - (1-V_p)t] \qquad \text{(AVII-9)}$$

and (47) gives

$$v_1|_0 = -\cos[x - (1-V_p)t] \qquad \text{(AVII-10)}$$

in the fixed frame. Substituting (AVII-9) and (AVII-10) into (AVII-8), we obtain

$$W = -\alpha^2 \int_0^{2n\pi} 4d \cos^2[x - (1-V_p)t] + O(\alpha^3)$$

or

$$W = -2\alpha^2 d + O(\alpha^3) \qquad \text{(AVII-11)}$$

The flow rate as given by equation (67) is

$$Q = \psi^+(y_s) + \psi^-(y_{\bar{w}}) - [\psi^+(y_w^+) + \psi^-(y_s)] \quad \text{(AVII-12)}$$

where ψ is a fixed frame quantity. Expanding (AVII-12) in a Taylor series about $y = 0$ and $y = \pm h$ and ψ in powers of α, we have to $0(\alpha^2)$

$$Q = \pm\alpha \left[\psi_1^{\pm}|_0 - \psi_1^{\pm}|_{\pm h} \right] \quad \text{(AVII-13)}$$
$$\pm\alpha^2 \left\{ \psi_2^{\pm}|_0 - \psi_2^{\pm}|_{\pm h} + \frac{\partial \psi_1^{\pm}}{\partial y}\Big|_0 \sin[x - (1-V_p)t] \right.$$
$$\left. \mp\beta \frac{\partial \psi_1^{\pm}}{\partial y}\Big|_{\pm h} \sin m[x - \gamma t] \right\}$$

From the boundary conditions (47), we find

$$\frac{\partial \psi_1^{\pm}}{\partial y}\Big|_0 = 0$$
$$\frac{\partial \psi_1^{\pm}}{\partial y}\Big|_{\pm h} = 0 \quad \text{(AVII-14)}$$

and from equation (52)

$$\psi_1^{\pm}|_0 = -\sin[x - (1-V_p)t] \quad \text{(AVII-15)}$$

$$\psi_1^{\pm}|_{\pm h} = -\{\cosh(h) + d[\sinh(h) - h\cosh(h)]$$
$$+ e\sinh(h)\} \sin[x - (1-V_p)t]$$
$$\mp\beta\gamma \{\tilde{F}\sin m[x-(1-V_p)t] + \tilde{G}\cos m[x-(1-V_p)t]\}$$
$$\{f[\sinh(mh) - mh\cosh(mh)]$$
$$+ g\, mh\sinh(mh)\}$$

$\psi_2^{\pm}$ in the fixed frame from (56) and (57) is

$$\psi_2^{\pm} = \text{SINE TERMS} + \text{COSINE TERMS} - \left(\frac{\ell}{2} - V_p\right) y \qquad \text{(AVII-16)}$$

Substituting (AVII-14) to (AVII-16) into (AVII-13) and averaging over the proper number of wavelengths, we obtain

$$\bar{Q} = 2h\alpha^2 \left(\frac{\ell}{2} - V_{p_2}\right) \qquad \text{(AVII-17)}$$

This is the desired flow rate.

Appendix VIII

The Analysis of Left Traveling Waves on the Wall

This analysis follows the same procedure as outlined previously. For the fixed frame (Frame 1), the wall shape is given by

$$y_{w1}^{\pm} = \pm h \pm \alpha\beta \sin m(x_1 + \gamma t) \qquad \text{(AVIII-1)}$$

The velocity of particles on the wall are

$$u_{w1}^{\pm} = 0, \quad v_{w1}^{\pm} = \pm \alpha\beta\gamma m \cos m(x_1 + \gamma t) \qquad \text{(AVIII-2)}$$

Moving to Frame 3, we find

$$u_{w3}^{\pm} = 0, \quad v_{w3}^{\pm} = \pm\alpha\beta\gamma m \cos m[x_3 + (\gamma + 1 - V_p)t] \qquad \text{(AVIII-3)}$$

The velocity of the sheet remains as in equation (16)

$$u_{s3}^{\pm} = 0, \quad v_{s3}^{\pm} = -\alpha \cos x_3 \qquad \text{(AVIII-4)}$$

and the boundary shapes are

$$y_{w3}^{\pm} = \pm h \pm \alpha\beta \sin m[x_3 + (\gamma + 1 - V_p)t]$$

$$y_{s3} = \alpha \sin x_3 \qquad \text{(AVIII-5)}$$

Expanding (AVIII-3) and (AVIII-5) by trigonometric identities yields

$$y_w^{\pm} = \pm h \pm \alpha\beta[\tilde{F}^* \sin mx + \tilde{G}^* \cos mx] \qquad \text{(AVIII-6)}$$

and

$$V_w^{\pm} = \pm \alpha \beta \gamma m \left[\tilde{F}^* \cos mx - \tilde{G}^* \sin mx \right] \tag{AVIII-7}$$

where

$$\tilde{F}^* = \cos(\gamma + 1 - V_p)t$$
$$\tilde{G}^* = \sin(\gamma + 1 - V_p)t$$

The boundary conditions become, as in (29), (30), and (31),

$$\left.\frac{\partial \psi_0^{\pm}}{\partial y}\right|_0 = 1$$

$$\left.\frac{\partial \psi_0^{\pm}}{\partial x}\right|_0 = 0 \tag{AVIII-8}$$

$$\left.\frac{\partial \psi_0^{\pm}}{\partial y}\right|_{\pm h} = 1 - V_{p_0}$$

$$\left.\frac{\partial \psi_0^{\pm}}{\partial x}\right|_{\pm h} = 0$$

$$\left.\frac{\partial \psi_1^{\pm}}{\partial y}\right|_0 = 0$$

$$\left.\frac{\partial \psi_1^{\pm}}{\partial x}\right|_0 = -\cos x$$

$$\left.\frac{\partial \psi_1^{\pm}}{\partial y}\right|_{\pm h} = -V_{P_1} \qquad \text{(AVIII-9)}$$

$$\left.\frac{\partial \psi_1^{\pm}}{\partial x}\right|_{\pm h} = \pm \beta \gamma m \left(\tilde{F}^* \cos mx - \tilde{G}^* \sin mx\right)$$

$$\left.\frac{\partial \psi_2^{\pm}}{\partial y}\right|_0 = -\left.\frac{\partial^2 \psi_1^{\pm}}{\partial y^2}\right|_0 \sin x$$

$$\left.\frac{\partial \psi_2^{\pm}}{\partial x}\right|_0 = -\left.\frac{\partial^2 \psi_1^{\pm}}{\partial x \partial y}\right|_0 \sin x \qquad \text{(AVIII-10)}$$

$$\left.\frac{\partial \psi_2^{\pm}}{\partial y}\right|_{\pm h} = -V_{P_2} \mp \beta \left.\frac{\partial^2 \psi_1^{\pm}}{\partial y^2}\right|_{\pm h} \left(\tilde{F}^* \cos mx + \tilde{G}^* \sin mx\right)$$

$$\left.\frac{\partial \psi_2^{\pm}}{\partial x}\right|_{\pm h} = \mp \beta \left.\frac{\partial^2 \psi_1^{\pm}}{\partial x \partial y}\right|_{\pm h} \left(\tilde{F}^* \cos mx + \tilde{G}^* \sin mx\right)$$

The derivatives of $\psi_0^{\pm}$ have been omitted in (AVIII-9) and (AVIII-10) since the boundary conditions of ψ_0 are identical with the previous solution, and we have

$$\psi_0^{\pm} = y \qquad \text{(AVIII-11)}$$

The boundary conditions for $\psi_1^{\pm}$ are similar to equations (47) with γ replaced by $-\gamma$. This leads to a stream function

$$\begin{aligned}\psi_1^{\pm} = -[&\cosh y \pm d(\sinh y - y\cosh y) \\ &+ e\, y \sinh y]\sin x \\ &+\beta\gamma(\tilde{F}^* \sin mx + \tilde{G}^* \cos mx) \\ [&f(\sinh my - my\cosh my) \\ &\pm g\, my \sinh my]\end{aligned} \qquad \text{(AVIII-12)}$$

where d, e, f, and g are given in (53).

The boundary conditions necessary for determining V_{p2} are

$$\left.\frac{\partial \psi_2^{\pm}}{\partial y}\right|_0 = -\frac{\ell}{2} + \text{SINE TERMS} + \text{COSINE TERMS}$$

(AVIII-13)

$$\left.\frac{\partial \psi_2^{\pm}}{\partial y}\right|_{\pm h} = -V_{p2} + \beta^2 \gamma m^2 \frac{\ell^*}{2} + \text{SINE TERMS} + \text{COSINE TERMS}$$

where ℓ and ℓ^* are found in (55). Following the arguments presented previously we find

$$V_{p2} = \frac{\ell}{2} + \beta^2 \gamma m^2 \frac{\ell^*}{2} \qquad \text{(AVIII-14)}$$

Similarly we find the energy in the fixed frame to be

$$W = -2\alpha^2 d \qquad \text{(AVIII-15)}$$

and the flow rate is given by

$$\bar{Q} = -h\, a^2 \beta^2 m^2 \gamma\, \ell^* \qquad \text{(AVIII-16)}$$

Appendix IX

The Analysis of Standing Waves on the Wall

Following the previous analysis of the right traveling wave, the boundary shapes for standing waves in the fixed frame are given by

$$y_{w_1}^{\pm} = \pm h \pm \alpha\beta \sin m x_1 \cos m\gamma t \qquad \text{(AIX-1)}$$

This gives rise to wall particle velocities of

$$u_{w_1}^{\pm} = 0 \;, \quad v_{w_1}^{\pm} = \mp \alpha\beta\gamma m \sin m x_1 \sin m\gamma t \qquad \text{(AIX-2)}$$

In Frame 3, we have

$$u_{w_3}^{\pm} = V_p - 1 \qquad \text{(AIX-3)}$$

$$v_{w_3}^{\pm} = \mp \alpha\beta\gamma m \sin m[x_3 + (1 - V_p)t] \sin m\gamma t$$

and the sheet particle velocities are (16)

$$u_{s_3}^{\pm} = -1 \;, \quad v_{s_3}^{\pm} = -\alpha \cos x_3 \qquad \text{(AIX-4)}$$

The boundary shapes transform to

$$y_{w_3}^{\pm} = \pm h \pm \alpha\beta \sin m[x_3 - (1 - V_p)t] \cos m\gamma t$$

$$y_s = \alpha \sin x_3 \qquad \text{(AIX-5)}$$

We now expand the velocities (AIX-3) and boundary shapes (AIX-5) using trigonometric identities

$$V_W^{\pm} = \mp \frac{1}{2} \alpha\beta\gamma m \{ \sin mx [\sin m(1-V_p+\gamma)t - \sin m(1-V_p-\gamma)t] + \cos mx [\cos m(1-V_p-\gamma)t - \cos m(1-V_p+\gamma)t] \} \quad \text{(AIX-6)}$$

The bracketed quantities are seen to be

$$\frac{\tilde{G}-\tilde{G}^*}{2} = -\frac{1}{2}[\sin m(1-\gamma-V_p)t - \sin m(\gamma+1-V_p)t] \quad \text{(AIX-7)}$$

$$\frac{\tilde{F}-\tilde{F}^*}{2} = \frac{1}{2}[\cos m(1-\gamma-V_p)t - \cos m(\gamma+1-V_p)t]$$

Then (AIX-6) becomes

$$V_W^{\pm} = \mp \alpha\beta\gamma m \left[\left(\frac{\tilde{F}-\tilde{F}^*}{2}\right)\cos mx - \left(\frac{\tilde{G}-\tilde{G}^*}{2}\right)\sin mx\right] \quad \text{(AIX-8)}$$

The wall shape also expands to give

$$y_W^{\pm} = \pm h \pm \alpha\beta \left[\left(\frac{\tilde{F} + \tilde{F}^*}{2} \right) \sin mx + \left(\frac{\tilde{G} + \tilde{G}^*}{2} \right) \cos mx \right] \tag{AIX-9}$$

This gives rise to the following boundary conditions,

$$\left. \frac{\partial \psi_0^{\pm}}{\partial y} \right|_0 = 1$$

$$\left. \frac{\partial \psi_0^{\pm}}{\partial x} \right|_0 = 0$$

$$\left. \frac{\partial \psi_0^{\pm}}{\partial y} \right|_{\pm h} = 1 - V_{p_0} \tag{AIX-10}$$

$$\left. \frac{\partial \psi_0^{\pm}}{\partial x} \right|_{\pm h} = 0$$

$$\left. \frac{\partial \psi_1^{\pm}}{\partial y} \right|_0 = 0$$

$$\left. \frac{\partial \psi_1^{\pm}}{\partial x} \right|_0 = -\cos x$$

$$\left. \frac{\partial \psi_1^{\pm}}{\partial y} \right|_{\pm h} = -V_{p_1} \tag{AIX-11}$$

$$\left. \frac{\partial \psi_1^{\pm}}{\partial x} \right|_{\pm h} = \mp \beta\gamma m \left[\left(\frac{\tilde{F} - \tilde{F}^*}{2} \right) \cos mx - \left(\frac{\tilde{G} - \tilde{G}^*}{2} \right) \sin mx \right]$$

$$\left.\frac{\partial \psi_2^{\pm}}{\partial y}\right|_0 = -\left.\frac{\partial^2 \psi_1^{\pm}}{\partial y^2}\right|_0 \sin x$$

$$\left.\frac{\partial \psi_2^{\pm}}{\partial x}\right|_0 = -\left.\frac{\partial^2 \psi_1^{\pm}}{\partial x \partial y}\right|_0 \sin x$$

(AIX-12)

$$\left.\frac{\partial \psi_2^{\pm}}{\partial y}\right|_{\pm h} = -V\rho_2 \mp \beta \left.\frac{\partial^2 \psi_1^{\pm}}{\partial y^2}\right|_{\pm h} \left[\left(\frac{\tilde{F}+\tilde{F}^*}{2}\right) \sin mx + \left(\frac{\tilde{G}+\tilde{G}^*}{2}\right) \cos mx\right]$$

$$\left.\frac{\partial \psi_2^{\pm}}{\partial x}\right|_{\pm h} = \mp \beta \left.\frac{\partial^2 \psi_1^{\pm}}{\partial x \partial y}\right|_{\pm h} \left[\left(\frac{\tilde{F}+\tilde{F}^*}{2}\right) \sin mx + \left(\frac{\tilde{G}+\tilde{G}^*}{2}\right) \cos mx\right]$$

The $\psi_0^{\pm}$ solution is given by (44)

$$\psi_0^{\pm} = y \qquad \text{(AIX-13)}$$

We find that the boundary conditions (AIX-11) are similar to equations (47) with F and G replaced by $\frac{F-F^*}{2}$ and $\frac{G-G^*}{2}$. By analogy $\psi_1^{\pm}$ is

$$\psi_1^{\pm} = -\left[\cosh y \pm d(\sinh y + y \cosh y) + e\, y \sinh y\right] \sin x \qquad \text{(AIX-14)}$$
$$-\beta r \left[\left(\frac{\tilde{F}-\tilde{F}^*}{2}\right) \sin mx + \left(\frac{\tilde{G}-\tilde{G}^*}{2}\right) \cos mx\right]$$
$$\left[f(\sinh my - my \cosh my) \pm g\, my \sinh my\right]$$

with d, e, f, g being given by (53).

From (AIX-12) the boundary conditions needed to determing V_{p_2} are found to be

$$\left.\frac{\partial \psi_2^{\pm}}{\partial y}\right|_0 = -\frac{\ell}{2} + \text{SINE TERMS} + \text{COSINE TERMS} \qquad \text{(AIX-15)}$$

$$\left.\frac{\partial \psi_2^{\pm}}{\partial y}\right|_{\pm h} = -V_{p_2} - \beta^2 \gamma m^2 \ell^* \left[\left(\frac{\tilde{F}^2 - \tilde{F}^{*2}}{4} \right) \sin^2 mx + \left(\frac{\tilde{G}^2 + \tilde{G}^{*2}}{4} \right) \cos^2 mx \right] + \text{SINE TERMS} + \text{COSINE TERMS}$$

Expanding the sine squared and cosine squared terms in (AIX-15) we obtain

$$\left.\frac{\partial \psi_2^{\pm}}{\partial y}\right|_{\pm h} = -V_{p_2} - \frac{1}{8} \beta^2 \gamma m^2 \ell^* \left[(\tilde{F}^2 - \tilde{F}^{*2}) + (\tilde{G}^2 - \tilde{G}^{*2}) \right] + \text{SINE TERMS} + \text{COSINE TERMS} \qquad \text{(AIX-16)}$$

and the bracketed quantity is zero from the definitions of F, G, F^* and G^*. This gives a propulsive velocity of

$$V_{p_2} = \frac{\ell}{2} \qquad \text{(AIX-17)}$$

Following the previous analogy, we find the energy in the fixed frame to be

$$W = -2a^2 d \qquad \text{(AIX-18)}$$

and the flow rate is

$$\bar{Q} = 0 \qquad \text{(AIX-19)}$$

It is interesting to note that the boundary conditions (AIX-11) are the superposition of the right and left traveling waves of one-half amplitude. The above results (to second order) could have been obtained by superposing the two previous solutions.